

# Comparison of phase-field models for surface diffusion

Clemens Müller-Gugenberger

*Institut für Festkörperforschung, Forschungszentrum Jülich, D-52425 Jülich, Germany*

Robert Spatschek

*Center for Interdisciplinary Research on Complex Systems,  
Northeastern University, Boston, MA 02115, USA and*

*Institut für Festkörperforschung, Forschungszentrum Jülich, D-52425 Jülich, Germany*

Klaus Kassner

*Institut für Theoretische Physik, Otto-von-Guericke-Universität Magdeburg, Postfach 4120, D-39016 Magdeburg, Germany*

(Dated: 10 November 2007)

The description of surface-diffusion controlled dynamics via the phase-field method is less trivial than it appears at first sight. A seemingly straightforward approach from the literature is shown to fail to produce the correct asymptotics, albeit in a subtle manner. Two models are constructed that approximate known sharp-interface equations without adding undesired constraints. Linear stability of a planar interface is investigated for the resulting phase-field equations and shown to reduce to the desired limit. Finally, numerical simulations of the standard and a more sophisticated model from the literature as well as of our two new models are performed to assess the relative merits of each approach. The results suggest superior performance of the new models in at least some situations.

PACS numbers: 68.35.Fx Surface diffusion; 02.70.-c Computational techniques; 47.20.Hw Morphological instability, phase changes

Keywords: Surface diffusion, phase-field model, tensorial mobility

## I. INTRODUCTION

For a large class of pattern-forming systems, the essential dynamics to be understood and described is that of an interface between two phases. Mathematically speaking, part of the problem to be solved consists in determining the position of the interface as a function of time, i.e., is a free or moving-boundary problem.

Phase-field models have been established as powerful tools for the numerical simulation of this kind of problem. They avoid explicit front tracking and are versatile enough to deal with topological changes. Phase-field methods constitute a special case of level-set approaches [1, 2]. They differ from the general case by having a level-set function that satisfies particular bulk equations of motion rendering unnecessary the computation of an extension of the interface velocity to the bulk. This way, they also avoid interface capturing at each time step, which is normally requisite in level-set methods. In comparison with other level-set methods, a drawback of the phase-field approach is that it does not yield an exact representation of the interface continuum problem, reducing to its dynamics only asymptotically. However, quantitative numerical control of phase-field representation has made enormous progress in the last decade [3, 4], so this disadvantage is not crucial anymore.

In a phase-field model, information on the interface position is present implicitly, given either as a level set of a particular value of the phase field (in two-phase models) or by equality of the phase-field values for different phases (in multi-phase models), and can be recovered by

computation of the appropriate level set at only those times when knowledge of the position is desired.

A major field of application are solidification problems, where diffuse-interface models were developed early on [5–7] and have seen renewed interest ever since computational power increased enough to render their simulation feasible. The concept was extended to anisotropic interface properties [8], and first qualitative numerical calculations of dendritic growth [9, 10] were followed by theoretical improvement of the asymptotics permitting quantitative simulations [3, 4], at least for intermediate to large undercoolings. Non-dendritic growth morphologies were also simulated, even in three dimensions [11]. Generalizations included the description of the coexistence of more than two phases [12, 13].

Additional examples of successful application of the tool phase field include the modeling of step-flow growth [14, 15] and of the elastically induced morphological instability [16–18], often labeled Grinfeld [19] or Asaro-Tiller-Grinfeld (ATG) instability [20]. All of the examples mentioned so far dealt with *nonconservative* interface dynamics, where a particle reservoir is provided by either the melt that is in contact with the solid or the adatom phase on a vicinal surface.

Actually, regarding the ATG instability, which is an instability with respect to material transport driven by elastic energy, interest initially focused on transport by surface diffusion, which leads to *conserved* dynamics. This was the case in the first article by Asaro and Tiller [20], but also in the first numerical simulations by sharp-interface continuum models [21], preceding computations of the instability under transport by melting-

crystallization [22].

The situation reversed when the phase-field method was employed for the first time to compute the ATG instability [16, 17]. Here, all the early works considered a nonconserved phase-field [16–18, 23]. Only recently has surface diffusion been considered in phase-field models treating elastically stressed materials [24, 25]. This difference in preferences when modeling either on the basis of a sharp-interface model or using a phase field may be due to the fact that writing down a nonconservative and a conservative model is equally simple in the former case, whereas it is less straightforward to write down the conservative model within the phase-field approach than the nonconservative one.

This is not to say that phase-field models with a conservation law for the phase field have not been considered at all. Starting from a Cahn-Hilliard equation with a concentration dependent mobility, Cahn et al. [26] obtained an interface equation with the normal velocity proportional to the Laplacian of the mean curvature. It then appears as if all phase-field models with surface diffusion should be derivable on the basis of similar considerations. Indeed, comparable models have been applied in the simulation of electromigration and voiding in thin metal films [27, 28]. These two models are slightly different, but the difference is not crucial and all previous models except the one given in [24] seem to suffer from the same problem, to be discussed in the following.

As we shall see, it is quite easy to set up a conservative phase-field model. But it is more difficult to obtain the correct asymptotics describing surface diffusion as given by the desired sharp-interface limit. Past models such as the ones presented in [25–28] while asymptotically producing a set of equations *containing* the desired limit equations, include an *additional restriction*, i.e., they have one equation too many, a fact that seems to have been overlooked so far. In [24], this restriction is not present, but the authors consider their improvement only a stabilizing element, not changing the asymptotics, whereas what they have achieved in reality is superior asymptotic behavior. Because the flaw of the faulty models is subtle, it is not a priori clear how adversely the undesired restriction will affect their behavior. Therefore, numerical simulations are necessary to assess their respective virtues and drawbacks.

The purpose of the present article is to demonstrate the overlooked restriction, to explore an alternative approach to phase-field modeling of surface diffusion, to derive additional models not having the aforementioned flaw, and finally, to compare the different models numerically.

To render things as simple as possible, we will restrict ourselves to two dimensions and give analytic derivations only for purely surface-diffusion-driven motion, i.e., the coupling to a destabilizing process such as elastic relaxation or electromigration will not be considered in the asymptotic analysis. The fully three-dimensional model including elastic energy and thus describing the ATG instability has been given in [29], an article with lower

pedagogical ambitions than this one. In simulations, we will consider both surface diffusion and elastic degrees of freedom, i.e., the ATG instability, to be able to make comparisons for stable and unstable situations.

The paper is organized as follows. In Sec. II, the sharp-interface model to be approximated by the phase-field equations is specified. The nonconservative case will be discussed for reference purposes. Section III then presents the standard approach that previously was supposed to reduce to the correct limit and pinpoints the oversight in existing asymptotic analyses. An alternative approach is presented in Sec. IV failing for complementary reasons. By appropriate combination of the ideas from both approaches, two phase-field models will be given in Sec. V producing the correct asymptotic behavior. An analytic linear stability analysis of these models shows, in Sec. VI, that they correctly reproduce the spectra of the sharp-interface limit. In Sec. VII, comparisons of the different models will be performed via numerical simulation for a number of pertinent situations. Finally, some conclusions to be drawn from both analytic and numerical calculations will be discussed.

## II. SHARP-INTERFACE MODEL FOR MOTION INDUCED BY CURVATURE

In the simplest case, where surface energy is the only relevant quantity determining the motion of an interface, the local chemical potential difference between the solid and the second phase [liquid, gas (vapour), or vacuum] at the interface may be written

$$\delta\mu = \frac{1}{\rho_s} \gamma\kappa, \quad (1)$$

where  $\rho_s$  is the density of the solid phase,  $\gamma$  the (isotropic) surface tension and  $\kappa$  the curvature (in 3D, the mean curvature). A positive curvature corresponds to a locally convex solid phase, a negative one to a locally concave solid.

Once the chemical potential is given, the stability of the interface can be assessed. From (1), we infer immediately that a planar interface is energetically stable. Any protrusion of the solid gives a convex bump and increases the energy of the solid over that of the second phase, leading to a nonequilibrium situation favoring diminution of the solid phase. Any indentation of the solid produces a concave bump and decreases the energy of the solid below that of the second phase, leading to a nonequilibrium situation favoring growth of the solid phase.

However, in order to determine the evolution of an unstable state, some dynamical law governing its motion must be stated. If a particle reservoir is present and the interface is rough, it is natural to assume linear nonequilibrium kinetics. The driving force then is the chemical potential difference itself, and the normal velocity  $v_n$  of the interface will be proportional to it:

$$v_n = -k_v \delta\mu, \quad (2)$$

where  $k_v$  is a mobility and the normal points from the solid into the second phase.

On the other hand, for material transport by surface diffusion, the driving force is the gradient of the chemical potential along the surface, producing a surface current  $j \propto -\nabla_s \delta\mu$  ( $\nabla_s$  is the surface gradient), which leads to a dynamical law of the form

$$v_n = M_s \Delta_s \delta\mu = M_s \frac{\partial^2 \delta\mu}{\partial s^2}, \quad (3)$$

where  $\Delta_s$  is the Laplace-Beltrami operator on the surface, reducing to a double derivative with respect to the arc length for a one-dimensional interface, and  $M_s$  a mobility coefficient (dimensionally different from the mobility  $k_v$ ), assumed constant here.

A linear stability analysis of a planar interface is readily performed, writing

$$\zeta(x, t) = \zeta_0 + \epsilon \zeta_1 e^{ikx + \omega t} \quad (4)$$

where  $\zeta_0$  is the constant position of the unperturbed interface,  $x$  the cartesian coordinate parallel to it, and  $\epsilon$  a small parameter used to keep track of orders of the perturbation expansion. The form of the perturbation, containing a wave number  $k$  and a growth rate  $\omega$ , is dictated by the fact that plane waves are eigenmodes of the differential operator  $\partial_x^2$  appearing in the definition of the curvature (5) and that  $v_n = \dot{\zeta}/[1 + (\partial_x \zeta)^2]^{1/2}$  is proportional to a first-order time derivative. Using

$$\kappa = -\frac{\partial_x^2 \zeta}{[1 + (\partial_x \zeta)^2]^{3/2}}, \quad (5)$$

one obtains the dispersion relations

$$\omega = -\frac{k_v \gamma}{\rho_s} k^2 \equiv -K k^2 \quad (6)$$

for the nonconservative and

$$\omega = -\frac{M_s \gamma}{\rho_s} k^4 \equiv -M k^4 \quad (7)$$

for the conservative cases, respectively. To arrive at the last result, note that to linear order (in  $\epsilon$ )  $\partial_x^2$  is not different from  $\partial_x^2$ .

For brevity, we have defined new kinetic coefficients  $K$  and  $M$ , which allows us to avoid carrying along the factor  $\gamma/\rho_s$  all the time.

The two models for motion by curvature considered here are given by Eqs. (1) and (2) on the one hand and Eqs. (1) and (3) on the other, describing the nonconservative and conservative cases, respectively. A phase-field model trying to represent these dynamics should converge to the appropriate set of these sharp-interface equations in the limit of asymptotically small interface width. More interesting and more complex physical problems are obtained, when the normal velocity depends on additional ingredients beyond curvature-induced driving forces. This will then lead to a coupling of the phase field to other fields. We shall discuss such a case later on.

### III. SCALAR-MOBILITY PHASE-FIELD MODEL

Before considering the structure of previous phase-field models attempting to capture surface diffusion dynamics, let us briefly recall the phase-field model for nonconserved order parameter  $\phi$ . This can be written [18]

$$\frac{\partial \phi}{\partial t} = K \left( \nabla^2 \phi - \frac{2}{W^2} f'(\phi) \right) \quad (8)$$

where  $f(\phi) = \phi^2(1 - \phi)^2$  is the usual double-well potential describing two-phase equilibrium.  $\phi$  varies between 0, corresponding to the nonsolid phase, and 1, corresponding to the solid;  $W$  measures the width of the transition region between the two phases, i.e., it may be interpreted as an interface thickness. A prime denotes a derivative with respect to the argument.

The standard approach to a phase-field description of surface diffusion, as proposed in [25–28], is then to prepend the right hand side of Eq. (8) with a differential operator corresponding to the divergence of a gradient multiplied by a phase-field dependent mobility, i.e., Eq. (8) becomes replaced with

$$\begin{aligned} \frac{\partial \phi}{\partial t} &= \nabla \cdot \mathbf{j} \\ \mathbf{j} &= \tilde{M} \nabla \frac{1}{W^2} \delta\tilde{\mu}(\nabla^2 \phi, \phi), \\ \delta\tilde{\mu}(\nabla^2 \phi, \phi) &\equiv -W^2 \nabla^2 \phi + 2f'(\phi) \end{aligned} \quad (9)$$

where  $\tilde{M}$  is a scalar function of either  $\phi$  [25, 26, 28] or  $W\nabla\phi$  [27], chosen such that the mobility tends to zero far from the interface:  $\tilde{M}(\phi, W\nabla\phi) \rightarrow 0$  for  $\phi \rightarrow 0$  and  $\phi \rightarrow 1$ .  $\delta\tilde{\mu}$  is a nondimensionalized chemical potential difference.

We will refer to the model described by Eqs. (9) as the *scalar-mobility model* or briefly *SM model* in the following.

At this point, a few remarks are in order. First, the field  $\phi$  is the density of a conserved quantity by construction, since the right hand side of (9) is written as a divergence. This is true for any (nonsingular) form of the mobility function  $\tilde{M}$ . Second,  $\delta\tilde{\mu}$  becomes zero for  $\phi \rightarrow 0$  and  $\phi \rightarrow 1$ , meaning that there is no diffusion in the bulk anyway. One might therefore wonder whether it is really necessary to choose a mobility that goes to zero in the bulk. The conservation law plus the absence of diffusion far from the interface should suffice to restrict transport to diffusion along the interface. In fact, we shall see that essentially the same asymptotic results are obtained no matter what the form of  $\tilde{M}$ , the only conditions to be imposed being positivity (for almost all values of  $\phi$  or  $\nabla\phi$ ) and boundedness. It is just easier to derive them if it is in addition assumed that  $\tilde{M}$  vanishes in the bulk. On the other hand, it will turn out that if a restriction imposed by the asymptotics is removed (or not yet satisfied in the temporal evolution of the system),  $\tilde{M}$  has to decay sufficiently fast inside the bulk for the limit to make sense.

This may be relevant for the behavior of the model before it reaches its asymptotic state.

Finally, the issue at present is not so much whether the dynamics is conservative but whether it does reduce to the sharp-interface model of Sec. II in the limit of an asymptotically vanishing interface thickness. To investigate this, we have to explicitly carry out the asymptotic analysis.

### A. Local coordinate system

The basic idea of the analysis is to expand all dynamical quantities in terms of the small parameter  $W$  describing the interface thickness, to solve for the phase field and to use the solution to eliminate its explicit appearance from the equations. To this end, the domain of definition of the field is divided into an outer region, where gradients of fields can be considered to be of order one and an inner region (close to the interface), where these gradients are of order  $1/W$ . The expansion in powers of  $W$  is rather straightforward in the outer domain, Eq. (9) can be taken as a starting point directly. As to the inner domain (and its matching with the outer region), it is useful to first transform to coordinates adapted to its geometry. Therefore, local coordinates  $r$  and  $s$  are introduced with  $r$  orthogonal to the interface (defined as the level set corresponding to  $\phi(x, z, t) = 1/2$ ) and  $s$  tangential to it.  $r$  is the signed distance from the interface and will be rescaled by a stretching transformation  $r = W\rho$  to make explicit the  $W$  dependence for the expansion,  $s$  is the arc length of the interface curve. Inner and outer solutions must satisfy certain matching conditions due to the requirement that they agree in the combined limit  $W \rightarrow 0$ ,  $\rho \rightarrow \pm\infty$ ,  $r \rightarrow 0$ . These conditions are given in App. A.

To obtain a set of basis vectors for our local coordinate system, we first write

$$\mathbf{r} = \mathbf{R}(s) + r\mathbf{n}(s), \quad (10)$$

where  $\mathbf{r}$  is the position vector of a point near the interface,  $\mathbf{R}$  the position of the interface itself, and  $\mathbf{n}$  the normal vector on it (oriented the same way as in the sharp-interface model, i.e., pointing out of the solid).

Given the coordinates, it is a trivial matter to write down a coordinate basis

$$\begin{aligned} \mathcal{E}_r &\equiv \frac{\partial \mathbf{r}}{\partial r} = \mathbf{n}(s), \\ \mathcal{E}_s &\equiv \frac{\partial \mathbf{r}}{\partial s} = \frac{\partial \mathbf{R}}{\partial s} + r \frac{\partial \mathbf{n}}{\partial s} = (1 + r\kappa)\mathbf{t}, \end{aligned} \quad (11)$$

which is orthogonal. (This is no longer automatically true in 3D [29].)  $\mathbf{t} = \partial \mathbf{R} / \partial s$  is the unit tangent vector to the interface, and  $\partial \mathbf{n} / \partial s = \kappa \mathbf{t}$  is one of the Frenet formulas [30], specialized to two dimensions.

From (11), we first obtain the metric coefficients  $g_{\alpha\beta} =$

$\mathcal{E}_\alpha \mathcal{E}_\beta$ , where  $\alpha, \beta \in \{r, s\}$ . The metric tensor reads

$$(g_{\alpha\beta}) = \mathbf{g} = \begin{pmatrix} 1 & 0 \\ 0 & (1 + r\kappa)^2 \end{pmatrix}, \quad (12)$$

its determinant is

$$g \equiv \det \mathbf{g} = (1 + r\kappa)^2, \quad (13)$$

hence  $\sqrt{g} = 1 + r\kappa$  (using the locality of  $r$  to ascertain  $r\kappa < 1$ ), and the contravariant components of the metric tensor are obtained as

$$(g^{\alpha\beta}) = \mathbf{g}^{-1} = \begin{pmatrix} 1 & 0 \\ 0 & (1 + r\kappa)^{-2} \end{pmatrix}. \quad (14)$$

From now on, we use the Einstein summation convention for pairs of covariant and contravariant indices. The vectors of the reciprocal basis are obtained from  $\mathcal{E}^\alpha = g^{\alpha\beta} \mathcal{E}_\beta$ :

$$\begin{aligned} \mathcal{E}^r &= \nabla r = \mathbf{n}(s), \\ \mathcal{E}^s &= \nabla s = \frac{1}{\sqrt{g}} \mathbf{t}, \end{aligned} \quad (15)$$

The gradient and divergence read

$$\begin{aligned} \nabla &= \mathcal{E}^\alpha \partial_\alpha, \\ \nabla \cdot \mathbf{A} &= \frac{1}{\sqrt{g}} \partial_\alpha (\sqrt{g} g^{\alpha\beta} A_\beta). \end{aligned} \quad (16)$$

Note that on the interface, the covariant component  $A_r$  is equal to the normal component  $A_n$ , but that  $A_s$  is related to the tangential component  $A_t$  by  $A_s = \sqrt{g} A_t$ , because  $\mathcal{E}^s$  is not normalized to one.

In the following, we will denote inner quantities by the uppercase letter corresponding to the lowercase letter denoting the outer quantity, whenever this is meaningful.

Since the interface will move in general and the coordinates  $r$  and  $s$  are defined with respect to the interface, there is also a transformation rule for the time derivative:

$$\partial_t f(x, z, t) = \partial_t F(r, s, t) - \mathbf{v} \nabla F(r, s, t), \quad (18)$$

where  $\mathbf{v}(s, t)$  is the interface velocity. Equation (18) exhibits that the time derivative in the comoving frame is a material derivative. In order to formulate the matching conditions concisely, we will occasionally also write the outer fields as functions of the variables  $r$  and  $s$  (without changing their naming letter, thus in this case adhering to the physicists' convention of using a letter for a physical quantity rather than a mathematical function).

## B. Inner equations

To render the scales of the different terms more visible, we rewrite Eqs. (16) and (17) in the form

$$\nabla = \frac{1}{W} \mathbf{n} \partial_\rho + \frac{1}{\sqrt{g}} \mathbf{t} \partial_s, \quad (19)$$

$$\nabla \cdot \mathbf{A} = \frac{1}{\sqrt{g}} \left( \frac{1}{W} \partial_\rho \sqrt{g} A_r + \partial_s \frac{1}{\sqrt{g}} A_s \right), \quad (20)$$

$$\sqrt{g} = 1 + W\rho\kappa. \quad (21)$$

Assuming, without loss of generality, that the tangential velocity of the interface vanishes, Eq. (9) takes the following form

$$\begin{aligned} \partial_t \Phi - \frac{1}{W} v_n \partial_\rho \Phi &= \nabla \cdot \tilde{M} \nabla \frac{1}{W^2} \delta \tilde{\mu}(\nabla^2 \Phi, \Phi), \\ \delta \tilde{\mu}(\nabla^2 \Phi, \Phi) &= - \frac{1}{\sqrt{g}} \partial_\rho \sqrt{g} \partial_\rho \Phi \\ &\quad - W^2 \frac{1}{\sqrt{g}} \partial_s \frac{1}{\sqrt{g}} \partial_s \Phi + 2f'(\Phi), \end{aligned} \quad (22)$$

with

$$\nabla \cdot \tilde{M} \nabla = \frac{1}{W^2} \frac{1}{\sqrt{g}} \partial_\rho \sqrt{g} \tilde{M} \partial_\rho + \frac{1}{\sqrt{g}} \partial_s \frac{1}{\sqrt{g}} \tilde{M} \partial_s. \quad (23)$$

Hence, the leading term of the inner equation (22) with the differential operator given by (23) is of order  $W^{-4}$ .

## C. Expansions, matched asymptotic analysis

To solve the outer and inner equations successively, we expand the phase field in both the outer and inner domains in powers of  $W$

$$\begin{aligned} \phi(x, z, t) &= \phi^{(0)}(x, z, t) + W \phi^{(1)}(x, z, t) \\ &\quad + W^2 \phi^{(2)}(x, z, t) \dots \end{aligned} \quad (24)$$

and

$$\begin{aligned} \Phi(r, s, t) &= \Phi^{(0)}(r, s, t) + W \Phi^{(1)}(r, s, t) \\ &\quad + W^2 \Phi^{(2)}(r, s, t) \dots \end{aligned} \quad (25)$$

We now proceed solving the outer and inner equations order by order.

### 1. Leading order

The leading-order outer equation for  $\phi$  is

$$\nabla \cdot \tilde{M} \nabla f'(\phi^{(0)}) = 0, \quad (26)$$

which is to be supplemented with the boundary conditions  $\phi^{(0)} = 1$  and  $\phi^{(0)} = 0$  at infinity in the regions where the system is solid and non-solid, respectively. If we regard (26) as a partial differential equation for the function

$f'(\phi^{(0)})$  (rather than for  $\phi^{(0)}$  itself), this boundary condition translates into  $f'(\phi^{(0)}) \rightarrow 0$  as  $|\mathbf{r}| \rightarrow \infty$ , which may be seen immediately from the explicit form of  $f'(\phi)$ , given in App. B. The new boundary condition is valid everywhere at infinity except possibly in a region with size of order  $W$ . For general  $\tilde{M}(\phi, W\nabla\phi)$ , the partial differential equation (26) is of course nonlinear. Nevertheless, it can be shown to have the unique solution  $f'(\phi^{(0)}) = 0$ , if  $\tilde{M}$  is positive everywhere, except possibly on a set of measure zero.

To see this, multiply Eq. (26) by  $f'(\phi^{(0)})$ , integrate over all of space and use Gauss's theorem:

$$\begin{aligned} 0 &= \int dV f'(\phi^{(0)}) \nabla \cdot \tilde{M} \nabla f'(\phi^{(0)}) \\ &= - \int dV \tilde{M} \left[ \nabla f'(\phi^{(0)}) \right]^2 + O(W), \end{aligned} \quad (27)$$

where the  $O(W)$  stands for the surface integral at infinity. (We will often use the nomenclature for three-dimensional systems, not distinguishing between surface integrals and boundary contour integrals; also we employ  $dV$  for the volume element of both two- and three-dimensional space.) If  $\tilde{M}$  is positive almost everywhere, we immediately get  $f'(\phi^{(0)}) = \text{const.}$ , and the boundary conditions require the constant to be zero. This conclusion remains of course unchanged, if  $\tilde{M}$  becomes zero only when  $\phi^{(0)}$  is zero or one – a standard choice [28] is  $\tilde{M}(\phi) \propto \phi^2(1 - \phi)^2$ .

Hence, the unique solution to the leading-order outer problem is, if we now consider it an equation for  $\phi^{(0)}$  again,  $\phi^{(0)} = 1$  in  $\Omega^-$  and  $\phi^{(0)} = 0$  in  $\Omega^+$ , where  $\Omega^\mp$  are those regions of space, separated by the interface(s), in which  $\lim_{|\mathbf{r}| \rightarrow \infty} \phi^{(0)} = 1$  and  $0$ , respectively. The solution  $\phi^{(0)} = \frac{1}{2}$ , still possible for the equation interpreted as an equation for  $f'(\phi^{(0)})$ , is excluded by the boundary conditions for  $\phi^{(0)}$ . (This argument presupposes that we have no domains that are not connected with infinity. For the interior of a closed interface, the solution  $\phi^{(0)} = 1/2$  would have to be excluded by a stability argument or by making reference to initial conditions.)

It is then seen by inspection that the outer equation is indeed solved to *all* orders by the solution under discussion. With the usual construction of coupling terms to, say, mechanical or electrical degrees of freedom [17, 27], this remains true for the full phase-field model including the coupling, as these terms are typically made to vanish in the bulk. So our statement, which has some importance as we shall see, is valid beyond the oversimplified “free” model considered here for the purpose of demonstration. Any deviation of the outer solution from  $\phi^{(0)}$  must be transcendentally small.

Therefore, we have  $\phi^{(1)} \equiv 0$ ,  $\phi^{(2)} \equiv 0$ , which provides us with partial boundary conditions for the inner solutions  $\Phi^{(1)}$ ,  $\Phi^{(2)}$ , and so on (see App. A). Moreover, only the inner problem needs to be considered beyond the leading order.

Because  $g = 1 + O(W)$ , the leading-order inner problem

becomes [see Eqs. (22) and (23)]

$$\partial_\rho \tilde{M}(\Phi^{(0)}) \partial_\rho [\partial_{\rho\rho} \Phi^{(0)} - 2f'(\Phi^{(0)})] = 0, \quad (28)$$

where  $\partial_{\rho\rho} = \partial_\rho^2$ . This can be integrated once to yield

$$\partial_\rho [\partial_{\rho\rho} \Phi^{(0)} - 2f'(\Phi^{(0)})] = \frac{c_1(s)}{\tilde{M}(\Phi^{(0)})}, \quad (29)$$

where  $c_1(s)$  is a function of integration. It is here that we have to follow different lines of arguments, depending on whether  $\tilde{M}$  approaches zero for  $\rho \rightarrow \pm\infty$ , which is the case for the mobilities assumed in [25, 26, 28], or whether it is just a bounded (and possibly constant) function of  $\phi$ . In the first case, we may immediately conclude  $c_1 = 0$ , because the right hand side of (29) must not diverge. In the second case, we obtain the same result by integrating (29) first and invoking the boundary conditions:

$$\partial_{\rho\rho} \Phi^{(0)} - 2f'(\Phi^{(0)}) = c_1(s) \int_0^\rho \frac{1}{\tilde{M}} d\rho + c_2(s). \quad (30)$$

Since  $\tilde{M}$  is bounded from above and positive, the integral will be larger in magnitude than  $\int_0^\rho 1/(\sup_\rho \tilde{M}) d\rho = \rho/\sup_\rho \tilde{M}$ , so the two factors multiplying  $c_1$  and  $c_2$  are linearly independent. The left hand side approaches zero for  $\rho \rightarrow \pm\infty$  [the argument will be made more rigorous below in the discussion of  $\Phi^{(1)}$ ], so both  $c_1$  and  $c_2$  must be equal to zero. To argue that  $c_2$  is zero in the case where  $\tilde{M} \rightarrow 0$  for  $\rho \rightarrow \pm\infty$ , we can proceed the same way, except that we have already gotten rid of the term containing  $c_1$ , so the right hand side of (30) is  $c_2$  only.

To summarize, the leading-order inner equation results in

$$\partial_{\rho\rho} \Phi^{(0)} - 2f'(\Phi^{(0)}) = 0, \quad (31)$$

and this provides us with the solution  $\Phi^{(0)} = \frac{1}{2}(1 - \tanh \rho)$  as is shown in App. B.

## 2. Next-to-leading order

The next-to-leading order in Eq. (22) is the order  $W^{-3}$ . Since the differential operator in front of the chemical potential is of order  $W^{-2}$  and the chemical potential multiplied by another factor  $W^{-2}$ , we must expand  $\delta\tilde{\mu}$  up to order  $W$ . Equation (31) already tells us that  $\delta\tilde{\mu}^{(0)} = 0$ , so we obtain

$$\partial_\rho \tilde{M}(\Phi^{(0)}) \partial_\rho \delta\tilde{\mu}^{(1)} = 0, \quad (32)$$

from which we get

$$\partial_\rho \delta\tilde{\mu}^{(1)} = \frac{d_1(s)}{\tilde{M}(\Phi^{(0)})}. \quad (33)$$

As before, we can immediately conclude from this that  $d_1 = 0$ , if we assume  $\tilde{M}(\Phi^{(0)}) \rightarrow 0$  for  $\Phi^{(0)} \rightarrow 0, 1$ . For arbitrary but bounded  $\tilde{M}$ , we invoke the matching conditions (see App. A)

$$\lim_{\rho \rightarrow \pm\infty} \partial_\rho \delta\tilde{\mu}^{(1)} = \partial_r \delta\tilde{\mu}_{\text{out}}^{(0)}|_{\pm 0} = 0 \quad (34)$$

to obtain the same result (where for once we have denoted an outer quantity by a subscript "out").

Integrating once more with respect to  $\rho$  and writing out  $\delta\tilde{\mu}^{(1)}$ , we have

$$\begin{aligned} \delta\tilde{\mu}^{(1)} &= -\partial_{\rho\rho} \Phi^{(1)} - \kappa \partial_\rho \Phi^{(0)} + 2f''(\Phi^{(0)}) \Phi^{(1)} \\ &= d_2(s). \end{aligned} \quad (35)$$

Up to this point, there is agreement between this and preceding asymptotic analyses [27], if not in all details of the procedure, so at least in the results.

Let us now try to determine the function of integration  $d_2(s)$ . A priori, there is no reason to use a procedure different from what we have done before. We know the limiting behavior for  $\rho \rightarrow \pm\infty$  for two of the four terms on the right hand side of (35):  $\lim_{\rho \rightarrow \pm\infty} \partial_\rho \Phi^{(0)} = 0$  [which follows from either the matching conditions or by inspection of the solution (B8)] and  $\lim_{\rho \rightarrow \pm\infty} d_2(s) = d_2(s)$  (because  $d_2$  is independent of  $\rho$ ). Moreover, from the matching conditions, we obtain the limit for  $\Phi^{(1)}$

$$\begin{aligned} \Phi^{(1)} \sim \rho \phi^{(0)}(\pm 0) + \phi^{(1)}(\pm 0) &= \phi^{(1)}(\pm 0) = 0 \\ (\rho \rightarrow \pm\infty). \end{aligned} \quad (36)$$

The second equality follows from the fact that  $\phi^{(0)} = 0$  or  $\phi^{(0)} = 1$ , hence its derivative with respect to  $r$  vanishes on both sides of the interface; the third equality is a consequence of the fact that  $\phi^{(0)}$  solves the outer equation to all orders and hence  $\phi^{(1)} \equiv 0$ . In addition, it can be shown [29] that if the interaction with mechanical degrees of freedom is included, this will only lead to terms that also vanish in the limit  $\rho \rightarrow \pm\infty$ .

With three of the four terms in (35) having a definite limit, we may conclude that the fourth must have a limit as well and obtain

$$\lim_{\rho \rightarrow \pm\infty} -\partial_{\rho\rho} \Phi^{(1)} = d_2(s). \quad (37)$$

But if this limit exists, it cannot be different from zero: transforming to  $\xi = 1/\rho$ , we see that  $\partial_{\rho\rho} \Phi^{(1)} = (\xi^2 \partial_\xi^2)^2 \Phi^{(1)}$ , which implies the asymptotic behavior  $\Phi^{(1)} \sim -d_2/2\xi^2$  ( $\xi \rightarrow 0$ ) and hence the divergence of  $\Phi^{(1)}$  as  $-d_2\rho^2/2$ , if  $d_2 \neq 0$ . (The same kind of argument can be used to show that the left hand side of Eq. (30) goes to zero, even though the matching conditions do not provide a direct expression for  $\lim_{\rho \rightarrow \pm\infty} \partial_{\rho\rho} \Phi^{(0)}$ .)

The upshot of these detailed considerations is that

$$d_2(s) = \delta\tilde{\mu}^{(1)} = 0. \quad (38)$$

Previous treatments of the problem did not enter into these considerations. Instead, one of the following two equivalent approaches was chosen. Either, Eq. (35) was interpreted as a linear inhomogeneous differential equation for  $\Phi^{(1)}$  and Fredholm's alternative invoked. Since the appearing linear operator

$$\mathcal{L} = \partial_{\rho\rho} - 2f''(\Phi^{(0)}) \quad (39)$$

is hermitean, we know (from taking the derivative of Eq. (31) w.r.t.  $\rho$ ) that  $\partial_\rho \Phi^{(0)}$  is a solution to the adjoint homogeneous equation. The inhomogeneity of the differential equation must be orthogonal to this solution. Or else, Fredholm's alternative was not mentioned, the equation was simply multiplied by  $\partial_\rho \Phi^{(0)}$ , integrated, and it was shown via integration by parts that the terms containing  $\Phi^{(1)}$  disappear. Of course, this is the same thing.

We then obtain from (35)

$$-\int_{-\infty}^{\infty} \kappa (\partial_\rho \Phi^{(0)})^2 d\rho = \int_{-\infty}^{\infty} \partial_\rho \Phi^{(0)} d_2(s) d\rho = -d_2(s), \quad (40)$$

from which we get, using (B10),

$$d_2(s) = \frac{1}{3} \kappa. \quad (41)$$

Both Eqs. (38) and (41) were derived by valid methods, therefore they should both hold true. Nevertheless, as we shall see shortly, Eq. (38) is a quite undesirable result. This may be the deeper reason why it was so far overlooked and only the analog of Eq. (41) derived. When Eq. (38) is inserted in (41), it leads to zero curvature at lowest order. In a phase-field model for the ATG instability [29], the same kind of reasoning imposes a relationship between the elastic state of the material and the curvature. In models, where the interaction term is quadratic in  $W$  [27], it again imposes the restriction  $\kappa = O(W)$ . To summarize, in all cases we obtain a restriction on the curvature at lowest order, which means that the phase-field model will not be asymptotic as long as the deviation from this imposed value is not small.

### 3. Higher orders

To see that the model would indeed work if we did not have the restriction (38), let us consider the equations at the next two orders, ignoring for the time being the result  $d_2 = 0$ . Since both  $\delta\tilde{\mu}^{(0)} (= 0)$  and  $\delta\tilde{\mu}^{(1)}$  are independent of  $\rho$ , the first term of the operator (23) does not produce any contribution from these terms in (22), and the order  $W^{-2}$  equation reads

$$\partial_\rho \tilde{M} \partial_\rho \delta\tilde{\mu}^{(2)} + \partial_s \tilde{M} \partial_s \delta\tilde{\mu}^{(0)} = 0, \quad (42)$$

where we can immediately drop the second term, because of  $\delta\tilde{\mu}^{(0)} = 0$ . After two integrations this becomes

$$\delta\tilde{\mu}^{(2)} = e_1(s) \int_0^\rho \frac{1}{\tilde{M}} d\rho + e_2(s). \quad (43)$$

If  $\tilde{M} \rightarrow 0$  for  $\rho \rightarrow \pm\infty$ , we immediately find  $e_1(s) = 0$ . In the general case, we use the matching conditions [see (A6)]

$$\begin{aligned} \delta\tilde{\mu}^{(2)} \sim & \frac{1}{2} \rho^2 \partial_{rr} \delta\tilde{\mu}_{\text{out}}^{(0)}|_{r=\pm 0} + \rho \partial_r \delta\tilde{\mu}_{\text{out}}^{(1)}|_{r=\pm 0} \\ & + \delta\tilde{\mu}_{\text{out}}^{(2)}|_{r=\pm 0}. \end{aligned} \quad (44)$$

From Eq. (9), we gather that an expansion of  $\delta\tilde{\mu}_{\text{out}}$  in powers of  $W$  will contain three types of terms, the first of which have the form  $\nabla^2 \phi^{(k)}$  ( $k = 0, 1, \dots$ ), while the second contain factors  $\phi^{(k)}$  ( $k = 1, 2, \dots$ ), coming from an expansion of  $f'(\phi)$  about  $\phi^{(0)}$ , and the third include  $f'(\phi^{(0)})$  alone. All of these terms vanish, because  $\phi^{(k)} = 0$  for  $k > 0$  and because  $f'(\phi^{(0)}) = 0$ . This is simply a consequence of the fact that the outer equation is solved exactly by  $\phi^{(0)} = 0$  and  $\phi^{(0)} = 1$ . The ‘‘chemical potential’’ appearing in the phase-field equations needs to be related to the true, i.e., sharp-interface chemical potential only at the interface. In the outer domain, it is zero. We can then conclude from (44) that  $e_1(s) = 0$  (of course  $e_2(s) = 0$ , too, but we shall not make use of that result).

Given that  $\delta\tilde{\mu}^{(2)}$  is independent of  $\rho$ , the inner equation at order  $W^{-1}$  takes the form

$$-v_n \partial_\rho \Phi^{(0)} = \partial_\rho \tilde{M} \partial_\rho \delta\tilde{\mu}^{(3)} + \partial_s \tilde{M} \partial_s \delta\tilde{\mu}^{(1)}. \quad (45)$$

After integration over  $\rho$  ( $v_n$  does not depend on  $\rho$ ) we find

$$v_n = \partial_{ss} \delta\tilde{\mu}^{(1)} \int_{-\infty}^{\infty} \tilde{M}(\Phi^{(0)}) d\rho + \tilde{M}(\Phi^{(0)}) \partial_\rho \delta\tilde{\mu}^{(3)} \Big|_{-\infty}^{\infty}. \quad (46)$$

Here we can drop the second term on the right hand side, if  $\lim_{\rho \rightarrow \pm\infty} \tilde{M}(\Phi^{(0)}) = 0$ . Formally setting  $\int_{-\infty}^{\infty} \tilde{M}(\Phi^{(0)}) d\rho = 3M$  and using (41), we arrive at

$$v_n = M \partial_{ss} \kappa. \quad (47)$$

Hence, (47) reproduces the sharp-interface limit (3), with the relationship between  $M_s$  and  $M$  defined in (7).

Finally,  $M$  would be infinite for positive functions  $\tilde{M}(\Phi^{(0)})$  that do not reduce to zero for  $\rho \rightarrow \pm\infty$ ; therefore, in the end we would indeed have to require  $\tilde{M}(\Phi^{(0)})$  to decay far from the interface, if  $\delta\tilde{\mu}^{(1)}$  were different from zero. In reality, we do not just have (47), the equation we want, but in addition Eq. (38), requiring  $\delta\tilde{\mu}^{(1)} = 0$  and, consequently

$$v_n = 0. \quad (48)$$

At first sight, Eqs. (47) and (48) may look like contradicting each other, as we can prepare an initial state with arbitrary curvature of the interface, and hence the velocity should be different from zero according to (47) but equal to zero according to (48). However, in preparing an arbitrary initial state, we have no certainty that the system will already follow its (lowest-order) asymptotic dynamics. A similar phenomenon happens in *all* phase-field models when a simulation is started with an initial interface perturbed by white noise. Since the asymptotics of the phase-field equations require curvatures to be smaller than  $1/W$ , the initial stage of the dynamics where larger curvatures are present, will not be governed by these asymptotics. But in that case the asymptotic behavior is sufficiently robust to keep the initial stage short.

Since (48) is a lowest-order result for the interface velocity, we can conceive of two different scenarios. Either the next-order result for  $v_n$  is nonzero. Then the model might asymptotically reproduce the desired sharp-interface limit at the next order, but its utility would be restricted as it would be quantitative only for  $\kappa = O(W)$  (i.e.,  $\kappa W \ll W/L$ , where  $L$  is a typical system length scale such as, for example, the equilibrium diameter of a crystal). Its validity would be restricted to near-equilibrium situations. Or else  $v_n$  is zero at all orders of the asymptotic expansion, hence transcendentally small in the asymptotic limit. Again, this could describe a near-equilibrium situation at best. Moreover, such a model would violate the spirit of phase-field models in general, in which we seek to have an analytic statement about the sharp-interface limit with as short an expansion as possible. The necessity to perform asymptotics beyond all orders should not arise in problems where we have such a high degree of freedom in constructing the model equations.

As to the general behavior of the SM model, it is quite tempting to speculate that when conditions are such that (48) does not hold yet, the phase-field model discussed here will satisfy all the other less restrictive conditions already, including (47). Then the model would be applicable during the period where the influence of condition (38) leading to (48) is still small. However, it should be clear that without a theoretical estimate of the error in this not fully asymptotic state, the model can hardly be considered quantitative. Condition (38) should be expected to have a stabilizing influence on decaying modes of the interface, accelerating their relaxation towards equilibrium. Its effect on growing, i.e. unstable modes is difficult to assess.

It is instructive to note why the nonconservative model obtained when (9) is replaced with (8) does *not* suffer from a similar difficulty. In that model, the velocity is already determined at the next-to leading order. Instead of (35), we get

$$-v_n \partial_\rho \Phi^{(0)} = K \left\{ \partial_{\rho\rho} \Phi^{(1)} + \kappa \partial_\rho \Phi^{(0)} - 2f''(\Phi^{(0)}) \Phi^{(1)} \right\}. \quad (49)$$

Again we may conclude that all the terms on the right hand side go to zero as  $\rho$  is sent to  $\pm\infty$ . However, this does not lead to any constraints, since the left hand side is  $\rho$  dependent now and goes to zero as well, satisfying the limit automatically, whereas in the surface-diffusion case, it was a function of  $s$  only ( $d_2$ ) that could be concluded to be equal to zero. So consideration of the limit does not produce anything new here, and the only procedure available to extract information on  $v_n$  is to use Fredholm's alternative which gives the correct sharp-interface limit.

In the case of the nonconservative model, the introduced chemical potential functional is zero in the bulk just as in the conservative case, but there are no restrictions on its variation near the interface, where it acquires a form tending to a  $\delta$  function in the sharp-interface limit.

In the conservative model, this is excluded by restrictions on the derivative of the chemical potential with respect to  $\rho$ , meaning that the latter must be smooth across the interface. Since it is zero off the interface, it is zero on it as well. Due to this reason, the phase-field model strictly speaking applies only to the equilibrium limit. Far-from equilibrium dynamics is not likely to be captured faithfully.

Out of the phase-field models for surface diffusion considered in the literature, the only one that is (apart from our own work [29]) not subject to the criticism offered here seems to be the one given by Rätz, Ribalta, and Voigt [24]. Let us briefly discuss the asymptotics of this model that we will henceforth denote as the *RRV model*. In their simplest form, i.e., for isotropic surface tension and vanishing kinetic coefficient, the model equations read

$$\begin{aligned} \frac{\partial \phi}{\partial t} &= \nabla \cdot \mathbf{j} \\ \mathbf{j} &= MB(\phi) \nabla \frac{1}{W^2} \delta \hat{\mu}(\nabla^2 \phi, \phi), \\ \delta \hat{\mu} &= \frac{1}{g(\phi)} \left( -W^2 \nabla^2 \phi + 2f'(\phi) \right), \end{aligned} \quad (50)$$

with mobility function  $B(\phi) = 12\phi^2(1-\phi)^2$ , double-well potential  $f(\phi) = \phi^2(1-\phi)^2$ , and the so-called stabilizing function  $g(\phi) = 10\phi^2(1-\phi)^2$ . Here, we have rescaled the equations from [24] so as to obtain the same zeroth-order interface profile as in the SM model (with the original equations, the interface would have one third of the width of our profile). The leading-order inner problem becomes (31) again. At next-to leading order, we obtain  $\delta \hat{\mu}^{(1)} = d_2(s)$  (as before), but now the chemical potential function is defined differently – it has a prefactor that diverges in the bulk

$$\delta \hat{\mu}^{(1)} = \frac{1}{g(\Phi^{(0)})} \left( -\partial_{\rho\rho} \Phi^{(1)} - \kappa \partial_\rho \Phi^{(0)} + 2f''(\Phi^{(0)}) \Phi^{(1)} \right). \quad (51)$$

(The first-order term due to variation of the denominator vanishes, as it contains the differential expression from the left hand side of (31) as a factor.) The numerator of the right hand side of (51) goes to zero as  $\rho \rightarrow \pm\infty$  but so does the denominator  $g(\Phi^{(0)})$ , which renders  $\delta \hat{\mu}^{(1)}$  indefinite, thus introducing the degree of freedom necessary for a nonzero value  $d_2(s)$ . Multiplying the equation by  $g(\Phi^{(0)}) \partial_\rho \Phi^{(0)}$  and integrating with respect to  $\rho$  from  $-\infty$  to  $\infty$ , we arrive at

$$d_2 \int_{-\infty}^{\infty} g(\Phi^{(0)}) \partial_\rho \Phi^{(0)} d\rho = -\kappa \int_{-\infty}^{\infty} \left( \partial_\rho \Phi^{(0)} \right)^2 d\rho, \quad (52)$$

where use has been made of the fact that  $\Phi^{(0)}$  is a left null eigenvector of the linear operator [inside the parentheses in (51)] acting on  $\Phi^{(1)}$ , to get rid of the  $\Phi^{(1)}$  terms. The integrals in (52) are evaluated in App. B, they are equal to  $-1/3$  and  $1/3$ , respectively. Hence,  $d_2 = \kappa$ .



The steps for the following two orders of  $W$  follow precisely the scheme leading from (42) to (47), which then yields  $v_n = M^* \partial_{ss} \kappa$ , where  $M^* = \int_{-\infty}^{\infty} MB(\Phi^{(0)}) d\rho = M$  (for the integral see App. B), hence we obtain the desired sharp-interface limit (3).

Note that with this model, it is essential that the mobility function goes to zero off the interface. For the chemical potential  $\delta\hat{\mu}$  varies in the bulk (it behaves as  $d_2(s)$  near the interface), hence diffusion there must be suppressed by a vanishing mobility.

#### IV. TENSORIAL MOBILITY

While the RRV model avoids the mistake of imposing (38), it does so by a purely mathematical device, the introduction of the stabilizing function  $g(\phi)$ . It is then natural to ask whether an accurate model may not be derived on the basis of mainly physical considerations.

That the phase-field model given by Eq. (9) does not quite yield the correct asymptotics may be traced back to the fact that the differential operator  $\nabla \cdot \tilde{M} \nabla$ , prepended to the chemical potential, does not reduce to the surface Laplacian  $\Delta_s$  in the asymptotic limit. In fact, the second term on the right hand side of Eq. (23) is, up to a factor, the Laplace-Beltrami operator on the surface (for  $\rho = 0$ ), but the first term, containing derivatives with respect to  $\rho$  is orders of magnitude larger, being preceded by a factor of  $1/W^2$ . As a consequence, the asymptotics must be secured by the full solution of the equation rather than by both the operator and the chemical potential converging to the desired sharp-interface limits.

Realizing this property of the model, it seems natural to modify the differential operator via introduction of an essentially tensorial mobility. Let us denote by

$$\hat{\mathbf{n}} = -\frac{\nabla\phi}{|\nabla\phi|} \quad (53)$$

the normal on the surface  $\phi = \text{const.}$  (for  $\phi = 1/2$ , we have  $\hat{\mathbf{n}} = \mathbf{n}$ ), then we expect the operator  $\nabla \cdot P \nabla$  with

$$P = 1 - \hat{\mathbf{n}} : \hat{\mathbf{n}} \quad (54)$$

(cartesian components:  $P_{ij} = \delta_{ij} - \hat{n}_i \hat{n}_j$ ) to reduce to the surface Laplacian asymptotically. A colon is used to designate a dyadic product, so  $P$  is a projection operator projecting onto the tangential plane of a level set of  $\phi$ . Introducing the shorthand  $\phi_{,\alpha} = \partial_\alpha \phi$ , we have  $\nabla\phi = \mathcal{E}^\alpha \phi_{,\alpha}$  and

$$\begin{aligned} \nabla \cdot (1 - \hat{\mathbf{n}} : \hat{\mathbf{n}}) \nabla &= \\ \nabla \cdot \left( \mathcal{E}^\mu \partial_\mu - \frac{1}{(\nabla\phi)^2} \mathcal{E}^\alpha \phi_{,\alpha} g^{\beta\mu} \phi_{,\beta} \partial_\mu \right) &= \\ \frac{1}{\sqrt{g}} \partial_\nu \sqrt{g} g^{\nu\mu} \left( \partial_\mu - \frac{1}{(\nabla\phi)^2} \phi_{,\mu} g^{\alpha\beta} \phi_{,\alpha} \partial_\beta \right). \end{aligned} \quad (55)$$

The third expression is obtained from the second applying the divergence operator (17) and renaming  $\alpha \rightarrow \mu$ ,  $\beta \rightarrow \alpha$ ,  $\mu \rightarrow \beta$  in the three pairs of ‘‘mute’’ indices.

To expand this operator in powers of  $W$  in the inner domain, we introduce an abbreviation for a normalized gradient of  $\Phi$ , being of order  $W^0$ :

$$\begin{aligned} (\nabla\Phi)^2 &\equiv \frac{1}{W^2} (\tilde{\nabla}\Phi)^2, \\ (\tilde{\nabla}\Phi)^2 &= W^2 \Phi_{,\alpha} g^{\alpha\beta} \Phi_{,\beta} = \Phi_{,\rho}^2 + \frac{W^2}{g} \Phi_{,s}^2. \end{aligned} \quad (56)$$

Inserting this into (55) and carrying the expansion to formal order  $W^0$ , we find first that the order  $W^{-2}$  terms (containing two derivatives with respect to  $\rho$ ) cancel each other. The remainder reads

$$\begin{aligned} \nabla \cdot (1 - \hat{\mathbf{n}} : \hat{\mathbf{n}}) \nabla &= \\ \frac{1}{\sqrt{g}} \partial_\rho \frac{1}{\sqrt{g} (\tilde{\nabla}\Phi)^2} \left( \Phi_{,s}^2 \partial_\rho - \Phi_{,\rho} \Phi_{,s} \partial_s \right) &+ \\ + \frac{1}{\sqrt{g}} \partial_s \frac{1}{\sqrt{g}} \left( \partial_s - \frac{\Phi_{,\rho} \Phi_{,s}}{(\tilde{\nabla}\Phi)^2} \partial_\rho \right) &+ O(W), \end{aligned} \quad (57)$$

and this expression still contains derivatives with respect to  $\rho$ . However, *if* the leading-order solution  $\Phi^{(0)}$  depends on  $\rho$  only, as it did in the last section, then all the derivatives of  $\Phi$  with respect to  $s$  are  $O(W)$  at least, and since  $\sqrt{g} = 1 + O(W)$ , Eq. (57) reduces to  $\nabla \cdot (1 - \hat{\mathbf{n}} : \hat{\mathbf{n}}) \nabla = \partial_s^2 + O(W)$ , i.e., at leading order the operator indeed becomes the Laplace-Beltrami operator on the surface.

This then suggests to replace the phase-field equation (9) with

$$\frac{\partial\phi}{\partial t} = M \nabla \cdot (1 - \hat{\mathbf{n}} : \hat{\mathbf{n}}) \nabla \frac{1}{W^2} \delta\tilde{\mu}(\nabla^2\phi, \phi), \quad (58)$$

where  $\delta\tilde{\mu}$  is unchanged from (9) but  $M$  is a constant mobility now.

In this model, the equation for the velocity would appear at the next-to leading order already and take the form

$$v_n \partial_\rho \Phi^{(0)} = M \partial_{ss} \left\{ \partial_{\rho\rho} \Phi^{(1)} + \kappa \partial_\rho \Phi^{(0)} - 2f''(\Phi^{(0)}) \Phi^{(1)} \right\}. \quad (59)$$

Because the operators  $\mathcal{L}$  [defined in Eq. (39)] and  $\partial_{ss}$  commute, Fredholm’s alternative is applicable the same way as in the nonconservative case. This eliminates  $\Phi^{(1)}$  from the equation and produces the correct sharp-interface limit.

In spite of this enjoyable state of affairs, model (58) fails much more miserably than (9). The reason is that the zeroth-order solution is not unique. In fact, the leading-order outer equation

$$\nabla \cdot (1 - \hat{\mathbf{n}}^{(0)} : \hat{\mathbf{n}}^{(0)}) \nabla f'(\phi^{(0)}) = 0 \quad (60)$$

is solved by *any* (differentiable) function  $\phi^{(0)}$  satisfying the boundary conditions: obviously we have  $\nabla f'(\phi^{(0)}) = f''(\phi^{(0)}) \nabla\phi^{(0)}$ , whence

$$\begin{aligned} \hat{\mathbf{n}}^{(0)} : \hat{\mathbf{n}}^{(0)} \nabla f'(\phi^{(0)}) &= -\hat{\mathbf{n}}^{(0)} f''(\phi^{(0)}) |\nabla\phi^{(0)}| \\ &= f''(\phi^{(0)}) \nabla\phi^{(0)} = \nabla f'(\phi^{(0)}), \end{aligned} \quad (61)$$

which implies  $(1 - \hat{\mathbf{n}}^{(0)} : \hat{\mathbf{n}}^{(0)}) \nabla f'(\phi^{(0)}) = 0$  for all functions  $f'$  of  $\phi^{(0)}$ . Intuitively, this behavior can be easily understood for a planar interface. Then the equation of motion (58) strictly contains only derivatives of the phase field parallel to the interface, and the profile in the perpendicular direction therefore remains completely undetermined.

It can be said that this model fails for reasons complementary to those of the scalar model. Whereas we had one equation too many in that case, adding a constraint to the desired sharp-interface dynamics, now we have one equation too few, as there is nothing in the model fixing  $\phi^{(0)}$ . If we had the right  $\phi^{(0)}$ , the tensorial model would work perfectly.

## V. MODIFIED TENSORIAL MOBILITY MODELS WITH CORRECT ASYMPTOTICS

In order to obtain a model not plagued by either of the disadvantages of the two cases discussed, it appears that it is useful to combine ideas from both. While it is certainly desirable to have a differential operator that itself approaches the surface Laplacian, it should do so only for phase field functions that have the correct leading-order profile.

### A. Locally conservative model

One way to achieve this goal is to modify  $1 - \hat{\mathbf{n}} : \hat{\mathbf{n}}$  into

$$Q \equiv 1 - W^2 \frac{\nabla \phi : \nabla \phi}{4f(\phi)} = 1 - \frac{W^2 (\nabla \phi)^2}{4f(\phi)} \hat{\mathbf{n}} : \hat{\mathbf{n}}. \quad (62)$$

If we replace the projection operator in Eq. (58) by  $Q$ , then the *outer* equation at leading order will have the same differential operator as the scalar model with constant  $M$ .

On the other hand, in the *inner* domain, we have, *provided*  $\Phi^{(0)}$  solves the differential equation (B6),  $W^2 (\nabla \Phi)^2 = \Phi_{,\rho}^2 + O(W^2) = 4f(\Phi) + O(W)$  [this follows from Eqs. (56), (B7), and (B1)], whence  $Q \approx 1 - \hat{\mathbf{n}} : \hat{\mathbf{n}}$ .

This approximation is accurate up to  $O(W)$  only, which is not sufficient, because the order  $W$  correction would enter as a bothersome additive term in the next-to leading order inner equation.

A better inner approximation to  $1 - \hat{\mathbf{n}} : \hat{\mathbf{n}}$  than just  $Q$  is provided by a minor modification. Obviously, we have  $Q = 1 - \hat{\mathbf{n}} : \hat{\mathbf{n}} + O(W) \hat{\mathbf{n}} : \hat{\mathbf{n}}$  in the inner region. Taking this to some integer power  $m$  we get, because  $1 - \hat{\mathbf{n}} : \hat{\mathbf{n}}$  and  $\hat{\mathbf{n}} : \hat{\mathbf{n}}$  are orthogonal projectors:

$$Q^m = 1 - \hat{\mathbf{n}} : \hat{\mathbf{n}} + O(W^m) \hat{\mathbf{n}} : \hat{\mathbf{n}}. \quad (63)$$

These considerations lead us to make the ansatz

$$\begin{aligned} \frac{\partial \phi}{\partial t} &= M \nabla \cdot \mathbf{j} \\ \mathbf{j} &= Q^m \nabla \frac{1}{W^2} \delta \tilde{\mu} (\nabla^2 \phi, \phi), \\ \delta \tilde{\mu} &\equiv -W^2 \nabla^2 \phi + 2f'(\phi) \end{aligned} \quad (64)$$

and leave the precise choice of the value of  $m$  for later – it will be suggested by the asymptotic analysis.

The corresponding inner equations are

$$\begin{aligned} \partial_t \Phi - \frac{1}{W} v_n \partial_\rho \Phi &= M \nabla \cdot Q^m \nabla \frac{1}{W^2} \delta \tilde{\mu} (\nabla^2 \Phi, \Phi), \\ \delta \tilde{\mu} (\nabla^2 \Phi, \Phi) &= -\frac{1}{\sqrt{g}} \partial_\rho \sqrt{g} \Phi_{,\rho} \\ &\quad - W^2 \frac{1}{\sqrt{g}} \partial_s \frac{1}{\sqrt{g}} \Phi_{,s} + 2f'(\Phi), \end{aligned} \quad (65)$$

with

$$\begin{aligned} \nabla \cdot Q^m \nabla &= \frac{1}{\sqrt{g}} \partial_\nu \sqrt{g} g^{\nu\mu} \left\{ \partial_\mu - \left[ 1 - \left( 1 - \frac{W^2 (\nabla \Phi)^2}{4f(\Phi)} \right)^m \right] \right. \\ &\quad \left. \times \frac{1}{(\nabla \Phi)^2} \Phi_{,\mu} g^{\alpha\beta} \Phi_{,\alpha} \partial_\beta \right\}. \end{aligned} \quad (66)$$

#### 1. Leading order

In the outer equations,  $Q$  becomes the identity operator to leading order, i.e.,  $Q^{(0)}(\phi^{(0)}) = 1$ , and at the lowest order in  $W$ , we have

$$\nabla^2 f'(\phi^{(0)}) = 0, \quad (67)$$

a Laplace equation that we know to be uniquely solvable for  $f'(\phi^{(0)})$  with Dirichlet boundary conditions at infinity. This boundary condition is even homogeneous (except possibly in a part of the boundary region at infinity having a size of order  $W$ ), leading to the unique solution  $f'(\phi^{(0)}) \equiv 0$ . This leaves us with the three possibilities  $\phi^{(0)} = 0, \frac{1}{2}, 1$ , of which  $\phi^{(0)} = 0$  or  $\phi^{(0)} = 1$  are realized, according to the particular boundary condition on  $\phi^{(0)}$ .

Again,  $\phi = 0$  and  $\phi = 1$  are solutions to the outer problem at all orders of  $W$ . Admittedly, the operator  $Q$  becomes indefinite at order  $W^2$  for  $\phi = 0$  and  $\phi = 1$  [because of the denominator  $f(\phi)$ ], but this does not matter, since the expression for  $\delta \tilde{\mu}$  alone is zero already at  $\phi = 0$  and  $\phi = 1$ .

The leading-order inner equation reads [ $g = 1 + O(W)$ ]

$$\partial_\rho \left[ 1 - \frac{(\Phi_{,\rho}^{(0)})^2}{4f(\Phi^{(0)})} \right]^m \partial_\rho \left( \partial_{\rho\rho} \Phi^{(0)} - 2f'(\Phi^{(0)}) \right) = 0. \quad (68)$$

Clearly, this is solved by  $\Phi^{(0)} = \frac{1}{2} (1 - \tanh \rho)$ , which makes both the expression in brackets and in large parentheses

vanish. If we require  $m$  to be even, this solution is moreover unique (up to translations, which are eliminated by the requirement that the interface be at  $\rho = 0$ ). For as soon as we assume  $(\Phi_{,\rho}^{(0)})^2 \neq 4f(\Phi^{(0)})$ , the  $m$ th power of the bracket expression will be positive, allowing us to use similar arguments as in Sec. III C between Eqs. (28) and (31) to prove that  $\partial_{\rho\rho}\Phi^{(0)} - 2f'(\Phi^{(0)}) = 0$ , and hence the bracket expression must be zero, contrary to our assumption. Thus we do get a definite solution for  $\Phi^{(0)}$  from the inner equation, which moreover shows that at leading order of the inner expansion the second-order  $\rho$  derivatives of the operator  $\nabla \cdot \mathcal{Q}^m \nabla$  cancel each other.

## 2. Next-to-leading order

To simplify computations at the next order, we first expand  $\nabla \cdot \mathcal{Q}^m \nabla$  up to formal order  $W^0$ . This produces

$$\begin{aligned} \nabla \cdot \mathcal{Q}^m \nabla = & \\ & \frac{1}{\sqrt{g}} \partial_s \frac{1}{\sqrt{g}} \partial_s + \frac{1}{\sqrt{g}} \frac{1}{W^2} \partial_\rho \sqrt{g} \left( 1 - \frac{W^2 (\nabla \Phi)^2}{4f(\Phi)} \right)^m \partial_\rho \\ & - \frac{1}{\sqrt{g}} \partial_\rho \frac{1}{\sqrt{g}} \frac{\Phi_{,s}}{\Phi_{,\rho}} \partial_s - \frac{1}{\sqrt{g}} \partial_s \frac{1}{\sqrt{g}} \frac{\Phi_{,s}}{\Phi_{,\rho}} \partial_\rho \\ & + \frac{1}{\sqrt{g}} \partial_\rho \frac{1}{\sqrt{g}} \frac{\Phi_{,s}^2}{\Phi_{,\rho}^2} \partial_\rho + O(W), \end{aligned} \quad (69)$$

Given that  $\Phi^{(0)}$  is a function of  $\rho$  only, we realize that the third and fourth terms on the right hand side are  $O(W)$ , containing derivatives with respect to  $s$  of  $\Phi$ , the fifth is even  $O(W^2)$ , so these terms may be dropped immediately in an expansion up to  $O(1)$ . The second term on the right hand side owes its existence to the fact that  $\mathcal{Q}$  is not exactly the projection operator on  $\hat{\mathbf{n}}$  [note that no such term is present in Eq. (57)] and it has a prefactor of  $1/W^2$  due to the double derivative in  $\rho$ . This term which is desirable at leading order, because without it we would not have a determinate zeroth order solution  $\Phi^{(0)}$ , is somewhat disturbing at the next order. Since the order of this term is  $O(W^{m-2})$ , we can make it small by choosing  $m \geq 3$ , i.e., restricting ourselves to even  $m$  for the reasons discussed before, we set  $m = 4$ . Then the only remaining term on the right hand side of Eq. (69) up to order  $W^0$  is the first term, which is the desired surface Laplacian.

Using this result, we can write the next-to-leading (nontrivial) order inner equation

$$\begin{aligned} -v_n \partial_\rho \Phi^{(0)} &= M \partial_{ss} \delta \tilde{\mu}^{(1)}, \\ \delta \tilde{\mu}^{(1)} &= -\mathcal{L} \Phi^{(1)} - \kappa \partial_\rho \Phi^{(0)}, \end{aligned} \quad (70)$$

again with  $\mathcal{L}$  as given in Eq. (39).

Note that we actually seem to have skipped orders here. The leading-order inner equation is formally  $O(W^{-4})$ , but once the zeroth-order inner solution is fixed, the differential operator  $\nabla \cdot \mathcal{Q}^m \nabla$  is, according to (69), of

order  $W^{\max(0, m-2)}$  only, so the order  $W^{-3}$  vanishes identically. The order  $W^{-2}$  is satisfied automatically, because the zeroth-order chemical potential is zero; the next nontrivial order is  $W^{-1}$ . Alternatively, one may say that the effective leading order has become  $W^{-2}$ .

The total linear operator in front of  $\Phi^{(1)}$  becomes  $-\partial_{ss} \mathcal{L}$ . It is hermitian, because its hermitian factors commute. Hence,  $\partial_\rho \Phi^{(0)}$  is a left null eigenfunction. Multiplying (70) from the left by it, integrating with respect to  $\rho$  from  $-\infty$  to  $\infty$ , we obtain Eq. (47). This proves that the considered phase-field model based on a modified tensorial mobility has the correct asymptotic behavior for small  $W$ , neither overconstraining the system by adding, nor leaving it indeterminate by losing equations.

Clearly, Eq. (64) establishes a *local* conservation law for  $\phi$ , i.e., the rate of change of the integral of  $\phi$  over some control volume is given by the integral of the current  $\mathbf{j}$  associated with  $\phi$  over the surface of the volume, and this holds for *arbitrarily small* volumes.  $\phi$  is the density of a conserved quantity. In particular, for a system with boundaries through which there is no flux, the volume integral of  $\phi$  will be conserved. Therefore, we will denote the model discussed in this section as the *locally conservative tensorial* or *LCT model*.

## B. Globally conservative model

If one is willing to give up the conservative nature of the phase-field equations themselves and requires the conservation law only in the asymptotic limit, an even simpler construction is feasible.

Consider the model

$$\begin{aligned} \frac{\partial \phi}{\partial t} &= M \nabla \cdot P \nabla \frac{1}{W^2} \delta \tilde{\mu} + N \left[ (\hat{\mathbf{n}} \cdot \nabla)^2 \phi - \frac{2}{W^2} f'(\phi) \right] \\ P &= 1 - \hat{\mathbf{n}} : \hat{\mathbf{n}} \\ \delta \tilde{\mu} &= -W^2 \nabla^2 \phi + 2f'(\phi) \end{aligned} \quad (71)$$

with both  $M$  and  $N$  positive constants. With  $N = 0$ , this reduces to the tensorial model of Sec. IV. With  $N > 0$ , it can be shown along similar lines as in Sec. III C 1 that the leading-order outer solution for  $\delta \tilde{\mu}$  is unique leading to the solutions  $\phi = 0$  and  $\phi = 1$ , depending on the boundary conditions at infinity. Moreover, the leading-order inner solution with boundary conditions  $\lim_{\rho \rightarrow -\infty} \Phi^{(0)} = 0$ ,  $\lim_{\rho \rightarrow \infty} \Phi^{(0)} = 1$  can be shown to be unique up to translations along  $\rho$  and is given by (B8) after requiring  $\rho = 0$  to correspond to the value  $\frac{1}{2}$  of the phase field.

The role of the  $N$  term is only to fix the profile of the phase field at leading order, otherwise it is constructed so as to not affect the normal velocity of the interface. Once  $\Phi^{(0)}$  is set, the next-to-leading order inner equation reads:

$$(M \partial_{ss} - N) \mathcal{L} \Phi^{(1)} = v_n \partial_\rho \Phi^{(0)} - M \partial_{ss} \kappa \partial_\rho \Phi^{(0)}, \quad (72)$$

and since  $M \partial_{ss} - N$  commutes with  $\mathcal{L}$ , we obtain the desired sharp-interface limit again. Our numerical investigations indeed show that the results depend only weakly

on the choice of the parameter  $N$ , even for moderate separation of the length scales. We find  $N \leq 2.5M/W^2$  to already give satisfactory results – there are only small differences to results obtained when  $N$  is two orders of magnitude smaller, i.e., for  $N = 1.25 \times 10^{-2}M/W^2$ .

While the model (71) is asymptotically conservative, it is desirable to have exact global conservation of the phase-field, because this will render long-time simulations more reliable. As the model stands, one might be obliged to choose the interface width smaller as the simulation time becomes larger, which is certainly something one would wish to avoid. Therefore, even though the violation of phase-field conservation is small and the model would already be useful in its present form, let us look for an improvement restoring global conservation. By this we mean that  $\phi$  need not be the density of a conserved quantity, hence its time derivative need not be the divergence of a current, but for no-flux boundary conditions, the total volume integral of  $\phi$  should remain conserved. This can of course be achieved via the introduction of a Lagrange parameter:

$$\frac{\partial \phi}{\partial t} = M \nabla \cdot P \nabla \frac{1}{W^2} \delta \tilde{\mu} + N \left[ (\hat{\mathbf{n}} \cdot \nabla)^2 \phi - \frac{2}{W^2} f'(\phi) \right] - \Lambda(\mathbf{r}, t). \quad (73)$$

Here, we have allowed  $\Lambda$  to depend on  $\mathbf{r}$  which gives useful additional freedom for improvement of the model as we shall see immediately. If  $\Lambda$  were restricted to being a simple number, it would have to have the value

$$\begin{aligned} \Lambda &= \frac{1}{V} \int_V dV \frac{\partial \phi_{\text{old}}}{\partial t} \\ &= \frac{N}{V} \int_V dV \left[ (\hat{\mathbf{n}} \cdot \nabla)^2 \phi - \frac{2}{W^2} f'(\phi) \right], \end{aligned} \quad (74)$$

where  $\partial \phi_{\text{old}}/\partial t$  is the time derivative of the phase field according to (71) and  $V$  is the volume (or area, in 2D) of the system. Since the first term of the right hand side of (73) is conservative anyway, it drops out of the calculation of  $\Lambda$ , if no fluxes through the system boundary are present. A drawback of the formulation (74) is that it would lead to a modification of the phase field in the bulk from the equilibrium values 0 and 1, as soon as the Lagrange multiplier became nonzero. This can be avoided by taking advantage of the liberty to make  $\Lambda$  vary in space (i.e., we consider a whole set of Lagrange multipliers, not just one). If we take  $\Lambda$  of the form

$$\Lambda(\mathbf{r}, t) = \frac{|\nabla \phi|}{\int_V dV |\nabla \phi|} \int_V dV \left[ (\hat{\mathbf{n}} \cdot \nabla)^2 \phi - \frac{2}{W^2} f'(\phi) \right], \quad (75)$$

the global conservation law is restored without any modification of the bulk solutions. We will call the model described by Eqs. (73) and (75) the *globally conservative tensorial* or *GCT model*.

Of course, we have to verify that the introduction of the Lagrange parameter does not destroy the asymptotic validity of the model. Clearly, the parameter disappears

from the leading order of the equation; but the interface velocity is determined at next-to leading order, and in general one would expect  $\Lambda(\mathbf{r}, t)$  to contribute to the equation at that order. This turns out not to be the case and is due to the judicious choice of the form of the parameter, as we shall see now.

The next-to leading order inner equation can be written

$$\begin{aligned} (M \partial_{ss} - N) \mathcal{L} \Phi^{(1)} + N \frac{\partial_\rho \Phi^{(0)}}{\int dV \partial_\rho \Phi^{(0)}} \int dV \mathcal{L} \Phi^{(1)} \\ = v_n \partial_\rho \Phi^{(0)} - M \partial_{ss} \kappa \partial_\rho \Phi^{(0)}, \end{aligned} \quad (76)$$

and we are in the awkward situation that the linear operator acting on  $\Phi^{(1)}$  is not self-adjoint, so the application of Fredholm's alternative becomes nontrivial. However, the equation contains several terms  $\propto \partial_\rho \Phi^{(0)}$ , which suggests to have  $\mathcal{L}$  act on it, leading first to the much simpler equation

$$\mathcal{L}(N - M \partial_{ss}) \mathcal{L} \Phi^{(1)} = 0, \quad (77)$$

because  $\mathcal{L} \partial_\rho \Phi^{(0)} = 0$ . But here the operator acting on  $\Phi^{(1)}$  is semipositive, the operator sandwiched by the two  $\mathcal{L}$ s strictly positive. Hence, we may conclude that  $\mathcal{L} \Phi^{(1)} = 0$ . But then the left-hand side of (76) is zero, meaning that the linear equation is in fact homogeneous and the right-hand side has to vanish, too. This implies

$$v_n = M \partial_{ss} \kappa, \quad (78)$$

the sought-for asymptotic result for the interface velocity. It also implies that the Lagrange multiplier is  $O(1)$ , instead of  $O(W^{-1})$ , i.e., it is by a factor of the order of  $(W\kappa)^2$  smaller than the leading-order terms of the equation.

This supports what we can point out on the basis of numerical studies: for reasonable separation of length scales as they appear in typical simulations, the influence of the Lagrange parameter is negligibly small, at least for not too long time scales.

## VI. ANALYTIC LINEAR STABILITY ANALYSIS

A linear stability analysis of a stationary planar front may be useful in trying to differentiate between the models. Clearly, one should require that the spectrum obtained for the phase-field model reduces to that of the sharp-interface model [e.g., Eqs. (6) or (7)] in the limit of small interface width.

For simplicity, let us first consider the nonconservative model described by (8). A planar front solution is given by

$$\phi = \phi_0(z) = \Phi_0(Z) = \frac{1}{2} (1 - \tanh Z), \quad Z = \frac{z}{W} \quad (79)$$

Adding a small perturbation  $\delta\phi$ , i.e., setting  $\phi = \phi_0 + \delta\phi(x, z, t)$ , we obtain the linearized equation

$$\frac{\partial \delta\phi}{\partial t} = M \left( \nabla^2 - \frac{2}{W^2} f''(\phi_0) \right) \delta\phi. \quad (80)$$

Using the ansatz

$$\delta\phi(x, z, t) = \Psi(Z)e^{ikx + \omega t} \quad (81)$$

we obtain the eigenvalue problem

$$\omega\Psi = \frac{M}{W^2} (\partial_{ZZ} - W^2k^2 - 2f''(\Phi_0))\Psi. \quad (82)$$

While this is a linear problem, it is one that does not have constant coefficients, so an exact solution is not readily available. Instead, we must rely on asymptotic analysis again to make progress. However, as it turns out by reinserting the found eigenfunctions and eigenvalues into (82), the expansion provides exact results in this case. Details of the calculation are given in App. C. We find two branches of the spectrum with

$$\begin{aligned} \omega_a &= -\frac{4M}{W^2} - Mk^2, \\ \omega_b &= -Mk^2. \end{aligned} \quad (83)$$

For the first branch, the eigenfunction does not vanish as  $Z \rightarrow \pm\infty$ , for the second it does and moreover is proportional to  $\Phi'_0(Z)$ . As  $Wk \ll 1$ , any contribution of the perturbation containing the first eigenfunction will decay fast, leaving a remainder that decays with rate  $\omega_b$ , which corresponds to the dispersion relation of the sharp interface-limit, Eq. (6). Note also that if we assume our initial perturbation to describe a slightly perturbed planar front, i.e.,

$$\phi = \frac{1}{2} \{1 - \tanh[Z - \delta\zeta(x)]\}, \quad (84)$$

then we have

$$\delta\phi = -\frac{\partial\Phi_0}{\partial Z} \delta\zeta, \quad (85)$$

hence the perturbation is  $\propto \Phi'_0(Z)$ , so the relevance of the second eigenvalue is obvious.

With these preliminaries, the linear stability analysis of the LCT model becomes more or less trivial. Linearizing the equation of motion (64) about  $\phi_0$ , we obtain

$$\frac{\partial\delta\phi}{\partial t} = M\nabla Q_0^4 \nabla \left( -\nabla^2 + \frac{2}{W^2} f''(\Phi_0) \right) \delta\phi, \quad (86)$$

where

$$Q_0 = Q(\Phi_0) = 1 - \mathbf{e}_z : \mathbf{e}_z, \quad (87)$$

as the level set normals are in the  $z$  direction and  $W^2(\nabla\Phi_0)^2/4f(\Phi_0) = 1$ . But then  $Q_0^4 = Q_0$ , and  $\nabla Q_0^4 \nabla = \partial_z^2$ . Hence,

$$\frac{\partial\delta\phi}{\partial t} = M\partial_{xx} \left( \nabla^2 - \frac{2}{W^2} f''(\phi_0) \right) \delta\phi \quad (88)$$

and after inserting ansatz (81), one gets

$$\omega\Psi = \frac{Mk^2}{W^2} (\partial_{ZZ} - W^2k^2 - 2f''(\Phi_0))\Psi. \quad (89)$$

But this is the same eigenvalue problem as (82) with  $M$  replaced by  $Mk^2$ . So we obtain a two-branch dispersion relation again, this time with eigenvalues

$$\begin{aligned} \omega_a &= -\frac{4Mk^2}{W^2} - Mk^4, \\ \omega_b &= -Mk^4, \end{aligned} \quad (90)$$

which in the light of the preceding discussion is a reasonable result (the eigenvalue with large absolute value is negative and influences the dynamics for a short time only).

Analysing the GCT model is only slightly more involved, at least in the form without the Lagrangian multiplier. One first derives that, for a perturbation about  $\Phi_0$  the simplification

$$\delta(\hat{\mathbf{n}}\nabla)^2\phi = \frac{1}{W^2} \partial_{ZZ} \delta\phi \quad (91)$$

holds true. Then the linearization of Eq. (71) reads

$$\begin{aligned} \frac{\partial\delta\phi}{\partial t} &= M\partial_{xx} \left( -\nabla^2 + \frac{2}{W^2} f''(\Phi_0) \right) \delta\phi \\ &+ \frac{N}{W^2} (\partial_{ZZ} - f''(\Phi_0)) \delta\phi. \end{aligned} \quad (92)$$

After using the ansatz (81), one can cast the resulting eigenvalue problem into the form (see App. C)

$$(\omega - Nk^2)\Psi = \frac{Mk^2 + N}{W^2} (\partial_{ZZ} - W^2k^2 - 2f''(\Phi_0))\Psi. \quad (93)$$

This again has the same form as (82), now with  $M$  replaced by  $Mk^2 + N$  and  $\omega$  replaced by  $\omega - Nk^2$ , leading to

$$\begin{aligned} \omega_a &= -\frac{4(Mk^2 + N)}{W^2} - Mk^4, \\ \omega_b &= -Mk^4. \end{aligned} \quad (94)$$

Considering now the form *with* the Lagrangian multiplier, (73) with (75), we note that

$$\delta\Lambda = \frac{|\nabla\Phi_0|}{\int_V d^3x |\nabla\Phi_0|} \int_V d^3x \frac{1}{W^2} (\partial_{ZZ} - 2f''(\Phi_0)) \delta\phi, \quad (95)$$

which becomes zero, if we insert the eigenfunction  $\Phi'_0(Z)$  belonging to  $\omega_b$  (see App. C). So this eigenvalue, which is the relevant one, remains unchanged. We can no longer exactly calculate the other eigenvalue nor the corresponding eigenfunction, but we anticipate that this eigenvalue still behaves as  $1/W^2$  at leading order and is negative, so it does not dominate the asymptotic behavior.

Unfortunately, an analysis of the SM model along the same lines turns out to be much more complicated. This may be traced back to the fact that the mobility function vanishes in the outer domain, leaving no useful linearized outer equation. In fact, the outer equation formally becomes  $\partial_t \delta\phi = 0$ , saying that at linear order perturbations

will not decay at infinity. In reality, this means that linearization is not legitimate, as perturbations will decay via nonlinear relaxation – the leading-order nonlinearity is larger than the (vanishing) linear expression. An analysis of the linearized inner equation with the requirement that  $\delta\Phi \rightarrow 0$  for  $Z \rightarrow \pm\infty$  does not produce any solutions for eigenvalues assumed to diverge more slowly as  $1/W^4$  (or not at all). If the requirement  $\delta\Phi \rightarrow 0$  is given up, one may construct perturbation eigenfunctions, but these contain polynomially diverging terms at infinity. On the other hand, eigenvalues of the form  $\omega = \omega_{-4}/W^4 + \dots$  could not be investigated by asymptotic analysis, because with this assumption the lowest-order perturbative problem remains unsolvable analytically. Note, however, that one eigenvalue of the form  $\omega = -Mk^4 + O(W)$  has to be expected for any phase-field model trying to meaningfully approximate the sharp-interface dynamics (3).

It is tempting to speculate that the fact of an undesirable restriction arising from the asymptotic analysis of the SM model and the unfeasibility of asymptotic analysis in a linear stability calculation of the model have to do with each other. This fits nicely with the observation that the linearized RRV model does have a usable outer equation. While its mobility function  $B(\phi)$  is zero in the bulk as well, the presence of the stabilizing function  $g(\phi)$  prevents the reduction to a static result. Writing the model in one equation

$$\frac{\partial\phi}{\partial t} = M\nabla \cdot B(\phi)\nabla \frac{1}{g(\phi)} \left( -\nabla^2\phi + \frac{2}{W^2}f'(\phi) \right), \quad (96)$$

we can recast the differential operator in front of the parentheses

$$\begin{aligned} \nabla \cdot B(\phi)\nabla \frac{1}{g(\phi)} &= \nabla^2 \frac{B(\phi)}{g(\phi)} - \nabla \cdot (\nabla B(\phi)) \frac{1}{g(\phi)} \\ &= \frac{6}{5}\nabla^2 - \frac{12}{5}\nabla \cdot (1 - 2\phi) \frac{\nabla\phi}{\phi(1-\phi)}, \end{aligned} \quad (97)$$

and the last term remains regular. The linearized equation of motion then becomes

$$\frac{\partial\delta\phi}{\partial t} = \frac{6}{5}M \left[ \nabla^2 + \frac{4}{W^2}\partial_z(1 - 2\Phi_0) \right] \left( -\nabla^2 + \frac{2}{W^2}f''(\Phi_0) \right) \delta\phi, \quad (98)$$

which for  $|Z| \gg 1$  turns into

$$\frac{\partial\delta\phi}{\partial t} = \frac{6}{5}M \left[ \nabla^2 + \frac{4}{W}\text{sign}_z\partial_z \right] \left( -\nabla^2 + \frac{4}{W^2} \right) \delta\phi, \quad (99)$$

a perfectly sensible outer equation.

Because the inhomogeneous fourth-order linear differential equations resulting from (98) at successive steps of the expansion are difficult to solve (this is in part due to the linear operator being nonhermitian) and the impossibility of getting analytic results for the SM model necessitates a numerical investigation anyway, we will not pursue the analytic discussion of the RRV model any further. We have checked that  $\Phi'_0(Z)e^{ikx+\omega t}$  is not an exact solution to the linearized equation here, so it appears quite likely that the relevant branch of the dispersion relation contains  $W$  dependent corrections, i.e.  $\omega = -Mk^4 + aW^2$ .

## VII. NUMERICAL SIMULATIONS

To determine growth rates numerically, we simulate the temporal evolution of a planar front subject to a sinusoidal perturbation. This allows the empirical determination of the main branch of the dispersion relations of the models considered, i.e., of the largest eigenvalue ( $\omega_b$ ). Moreover, to assess the behavior of the models in a growth situation, we include the coupling to elastic fields, i.e., we simulate the Grinfeld instability. This is easily achieved by replacing the “free” chemical potential  $\delta\tilde{\mu}$  with one that includes the correct elastic energy contribution.

In particular, we set

$$\delta\tilde{\mu}(\nabla^2\phi, \phi) \equiv -W^2\nabla^2\phi + 2f'(\phi) + \frac{W}{3\gamma}h'(\phi)V_{\text{el}}, \quad (100)$$

with

$$V_{\text{el}} = (G - \tilde{G}) \sum_{i,j} u_{ij}^2 + \frac{\lambda - \tilde{\lambda}}{2} \left( \sum_k u_{kk} \right)^2, \quad (101)$$

where  $G = E/[2(1+\nu)]$  is the shear modulus or first Lamé constant,  $\lambda = E\nu/[(1+\nu)(1-2\nu)]$  the second Lamé constant in the solid phase and  $\tilde{G}$  and  $\tilde{\lambda}$  are the corresponding quantities in the second phase. If the second phase is a liquid,  $\tilde{G} = 0$ , if it is vacuum,  $\tilde{G} = \tilde{\lambda} = 0$ . From now on, we will focus on the vacuum case, as it is particularly interesting for diffusion along a free surface. Equation (100) was originally introduced as a phase-field model for two coherent solid phases in contact with each other in [31]. Moreover, it has been discussed in [18] that modeling a liquid (or vacuum) as a shear-free solid faithfully captures the physics of the system in spite of the property of formally coherent strains. This is essentially due to the fact that only the divergence of the strain tensor is a physically meaningful quantity in the shear-free phase.

By  $u_i$ , we denote the displacement field. In addition, equations for the strains  $u_{ij} = \frac{1}{2}(\partial u_i/\partial x_j + \partial u_j/\partial x_i)$  have to be provided, which are given by the mechanical equilibrium conditions for the generalized stress tensor  $\tilde{\sigma}_{ij}$

$$\sum_j \frac{\partial \tilde{\sigma}_{ij}}{\partial x_j} = 0, \quad \tilde{\sigma}_{ij} = h(\phi)\sigma_{ij}. \quad (102)$$

The function  $h(\phi)$  is defined in (B4) and  $\sigma_{ij}$  is related to  $u_{ij}$  via Hooke’s law

$$\sigma_{ij} = \frac{E}{1+\nu} \left( u_{ij} + \frac{\nu}{1-2\nu} \sum_k u_{kk} \delta_{ij} \right). \quad (103)$$

That this model produces the right coupling to elasticity in the sharp-interface limit has been shown in various places, e.g. in [18] und [29]. A similar modification of  $\delta\tilde{\mu}$  leads to the fully coupled RRV model [24].

To simulate the Grinfeld instability in a strip geometry, a dimensionless driving force  $F$  is defined as

$$F = \frac{\delta^2(\lambda + 2G)}{4\gamma L}, \quad (104)$$

with  $\delta$  being a fixed displacement by which the strip is elongated in the direction parallel to the interface. We use a square system of length  $L$  and uniform grid spacing  $\Delta x$ . The interface width, a purely numerical parameter, is chosen to be  $W = 5\Delta x$ . For a sinusoidal perturbation of a uniaxially strained surface by  $\delta y(x) = A_0 \sin(kx)$  we use a fixed wavenumber  $kL = 4\pi$  and a small amplitude  $A_0 k = \pi/20$ . To obtain a good separation of the characteristic wavelength of the pattern and the interface width, we use  $kW = 0.16$ . The imposed uniaxial stress is given in the figure caption for each case. After having determined the maximum admissible time step, as discussed below, we take as simulation time step  $\Delta t = 5 \cdot 10^{-4}(\Delta x)^4/M$  for the scalar models and  $\Delta t = 5 \cdot 10^{-3}(\Delta x)^4/M$  for the tensorial models. The Poisson ratio is chosen to be  $\nu = \lambda/[2(\lambda + G)] = 1/3$ . For the GCT model, we use  $N = 1.25M/W^2$ , and for the SM model the standard choice  $\tilde{M}(\phi) = 36M\phi^2(1 - \phi)^2$ . To minimize the influence of the boundaries, we use helical boundary conditions in the  $x$  direction for the displacement fields, i.e.  $u_x(L, y) = u_x(0, y) + \delta$ ,  $u_y(L, y) = u_y(0, y)$ .

Introducing the Griffith length  $L_G$

$$L_G = \frac{L(1 - \nu)^2}{8F(1 - 2\nu)}, \quad (105)$$

we can write the dispersion relation, i.e., the spectrum of the linear stability operator, as follows

$$\omega = M \left( \frac{k^3}{L_G} - k^4 \right), \quad (106)$$

meaning that we have unstable modes at small  $k$  ( $k < 1/L_G$ ) and stable ones at large  $k$  ( $k > 1/L_G$ ). To obtain the spectrum numerically, we vary  $L_G$  in the simulations.

We use the same algorithm as in [31], which even works for dynamic elasticity. But since we investigate the beginning of the Grinfeld instability, the observed interface velocities are very small in comparison to the speed of sound, and the equations effectively reduce to the static elastic case of Eq. (102).

While the SM model can be discretized in a relatively straightforward manner, some care has to be taken in the other models to avoid divisions by zero. This is rather harmless in the GCT model, where the problem only arises in the computation of the vectors  $\hat{\mathbf{n}}$  ( $|\nabla\phi|$  goes to zero far from the interface but is positive otherwise, so it is sufficient to ensure that the denominator of  $\hat{\mathbf{n}}$  does not become smaller than a small positive number). The main requirement in the RRV model is that  $g(\phi)$  should not be set exactly equal to zero.

In the LCT model, more attention has to be paid to the situation where  $f(\phi)$  becomes small, as will be discussed below.

Essentially, we make four types of comparison. First, we compare the time evolution of sinusoidal fronts (initialized with the correct width of the profile) for a number of imposed uniaxial stresses and obtain the linear stability spectrum numerically. Second, we increase the time

step in the simulation for given mesh size until we reach the maximum possible time step providing convergence to the correct interface dynamics and then compare the achieved values. Next, we initialize a planar profile with the wrong interface width and observe relaxation to a profile of the correct width. In a realistic simulation, slight deviations from the correct profile width may easily appear in an initial condition for a curved interface, as analytical expressions for constant-width profiles at arbitrary curvature are not readily available (even for an initial germ with a shape as simple as an ellipse it is not quite trivial to give such an expression). Any phase-field code should be robust against these local variations of the profile width and should have it relax to the correct value. Finally, we look at the evolution of an elliptical inclusion. Since the phase-field parameter is a conserved quantity, the ellipse should morph to a circle with the same area.

In Figs. 1 to 3, we show the temporal evolution of a sine profile starting with a prescribed amplitude for different values of the imposed uniaxial stress. The four models are compared directly with the sharp interface prediction resulting from Eq. (106). Fig. 1 exemplifies the stress-free case discussed analytically.

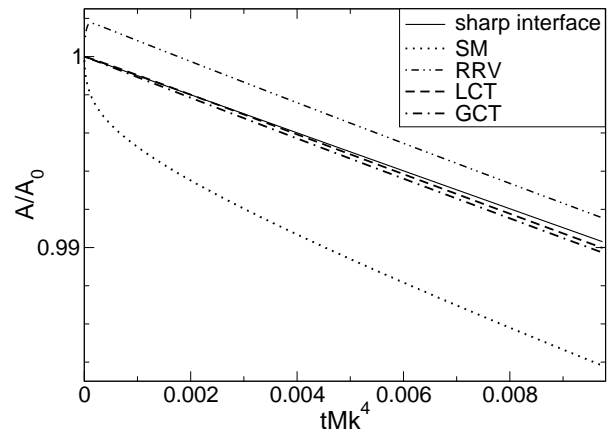


FIG. 1: Amplitude evolution for a uniaxial stress of  $F = 0$ , i.e., a Griffith length  $L_G = \infty$ .

All the situations considered correspond to either weak decay or weak growth of the amplitude, as the expected exponential behavior still appears linear on the considered time scale.

We note that all the models agree with the predicted behavior of the sharp-interface limit to within better than one percent for our parameters and time span. While it may be observed unambiguously that the SM model displays the largest deviation from the desired result, one may find it surprising that it reproduces the limit so well after all, taking into account that it does not have the right asymptotics. Presumably the general idea mentioned after Eq. (48) is not too far from the truth: those

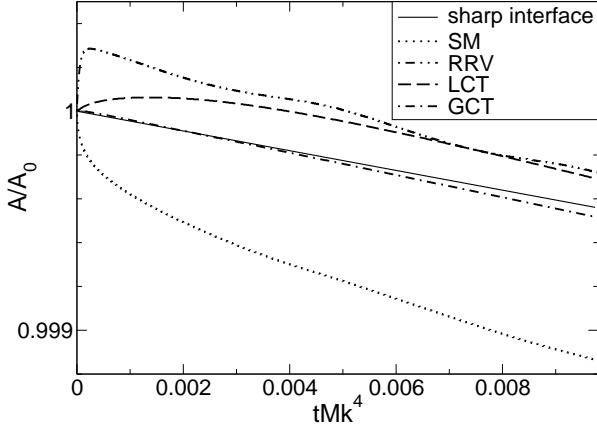


FIG. 2: Amplitude evolution for a uniaxial stress of  $F = 2$ .

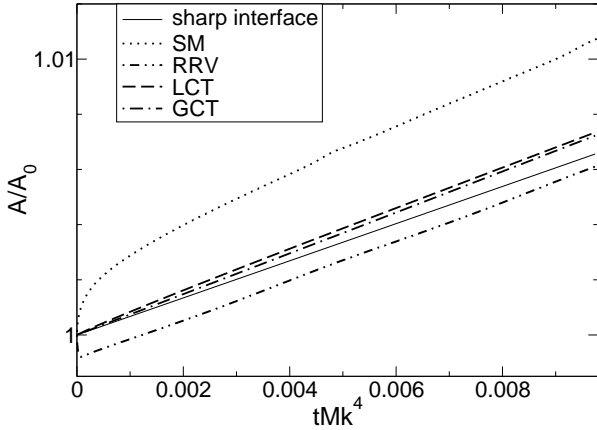


FIG. 3: Amplitude evolution for a uniaxial stress of  $F = 3.5$ .

equations of the asymptotic behavior to which the system can adjust locally act as an attractor for the dynamics even before the full set of equations, implying more global restrictions such as Eq. (48), becomes active. It is striking that this seems to work even in a growth situation, where interface velocities increase on average.

Figure 4 gives a comparison of the linear stability spectra, obtained by simulation of the four models, with the analytical expression Eq. (106) of the sharp-interface model. It is pretty clear that the SM model is farthest off the correct value both below and above the fastest-growing wavenumber. The LCT model is good for wavenumbers above that of the fastest-growing mode but shows stronger deviations than both the RRV and GCT model below that mode. The latter two models are about equally close to the correct spectrum throughout

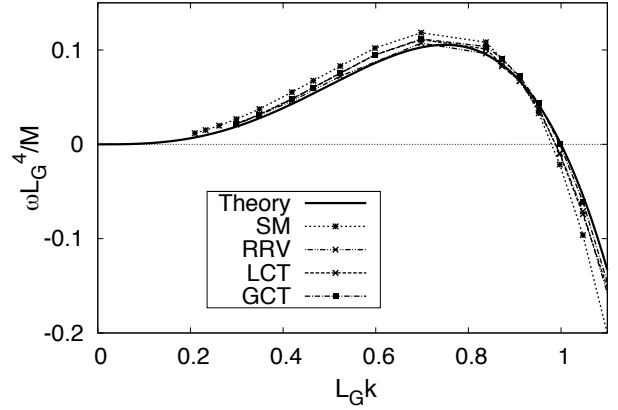


FIG. 4: Full spectrum of the ATG instability.

the whole wavenumber domain.

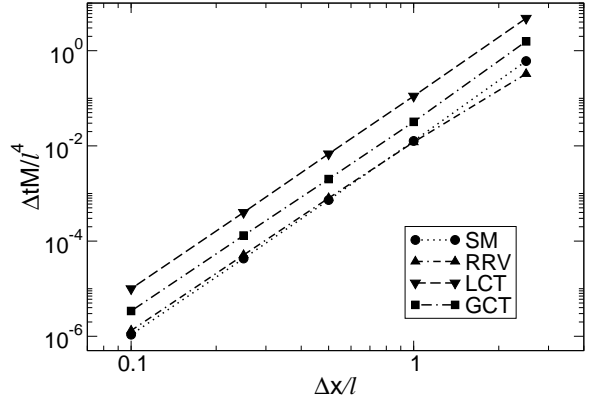


FIG. 5: Allowable maximal time step  $\Delta t$  as a function of mesh size, where  $l$  is an arbitrary length unit. Lines are a guide for the eyes only.

Fig. 5 displays the maximum time step for a given grid spacing leading to smooth growth where the results for all models agreed perfectly, independent of the time-discretization. We observe, for all models, a scaling of the maximum admissible time step as  $\Delta t \sim \Delta x^4 / M$ , which is not too surprising given the fact that the equations simulated are fourth order in space and first order in time, and we used straightforward explicit schemes for discretization. However, while in the two scalar models (SM, RRV) about the same maximum time step is possible, the tensorial models allow larger time steps; a simulation with the LCT model gains a factor of about ten in time steps over the scalar models. While by use of adaptive mesh techniques [24] (and implicit schemes),



the overall running time can certainly be reduced by more than this factor for large systems, the advantage of the tensorial models may persist even in such a setting as it is consistently present in a range of grid spacings.

Next, it is interesting to compare how the different models behave regarding their relaxation to a stationary profile when initialized with a straight interface having a width that is either too small or too large. These simulations are done without elasticity, i.e., for  $F = 0$ . First, we verify that all the models remain in their equilibrium state when initialized with a  $\tanh$  profile of the correct width.

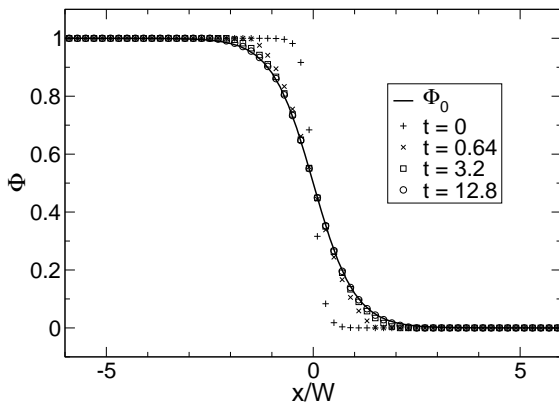


FIG. 6: Relaxation towards the correct interface profile for the SM model. The initial interface width is  $0.25 W$ , the time  $t$  is given in units of  $W^4/M$ .

For brevity of language, we define here a profile  $\tanh z/W$  to have width  $W$ , even when the width on which it rises from  $-0.9$  to  $0.9$  rather is  $2.94 W$ . In all plots, the time  $t$  is given in units of  $W^4/M$ , and only a small section about the interface is shown.

All of the models do reasonably well in relaxing from a planar profile of width  $0.25 W$  to their equilibrium state, see Figs. 6 to 9. In our implementation and with the given sets of parameters, simulations with the RRV model broke down if the initial interface width was chosen to be smaller than  $0.23 W$ . The RRV and GCT model relax quickly to a final profile of width  $W$ , while the SM model needs a little more time (but the permissible time *step* is larger for the GCT model, so the numerical running time is shortest for it). In addition, some care has to be taken in the discretization to make the LCT model deal efficiently with too thin interfaces.

To see this, we write  $Q^4 = 1 - \hat{\mathbf{n}} : \hat{\mathbf{n}} + b_0^4 \hat{\mathbf{n}} : \hat{\mathbf{n}}$  with

$$b_0 = 1 - \frac{W^2(\nabla\phi)^2}{4f(\phi)}. \quad (107)$$

Taking an interface of width  $\xi$  with the profile  $\phi(z) =$

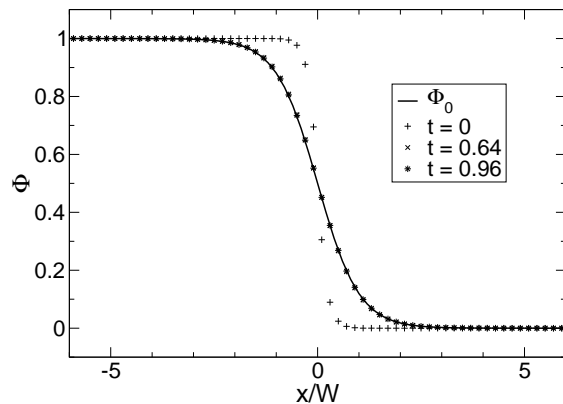


FIG. 7: Relaxation towards the correct interface profile for the RRV model. The initial interface width is  $0.25 W$ , the time  $t$  is given in units of  $W^4/M$ .

$\frac{1}{2}(1 - \tanh z/\xi)$  we find

$$b_0^4 = \left(1 - \frac{W^2}{\xi^2}\right)^4, \quad (108)$$

which becomes very large for  $\xi \ll W$ . In fact, for  $\xi = 0.25W$ , we have  $b_0^4 = 50625$ , a number that, when plugged into the equations of motion, would impose a prohibitively small time step for stability (or accuracy, in an implicit scheme). Hence, we introduce a cutoff for  $b_0^4$  on the order of 50. In production runs, where one normally starts with a front profile having at least approximately the correct width, a cutoff of 10 may be sufficient.

When the profile is initialized with too large a width [Figs. 10 through 13], more interesting differences can be seen. Not unexpectedly, the GCT model [Fig. 13] is the one making the least fuss about an interface five times too wide: that the model is nonconservative on the scale where the phase field varies strongly is an advantage here. The interface approaches its correct width in a time of about  $t \approx 1.25 W^2/N$ , which corresponds to  $t \approx 1 W^4/M$  for our parameter choice. For the other models, this takes much longer, as this kind of adaptation requires diffusion orthogonally to the front, which is slow because it is suppressed in the asymptotic limit.

The RRV model goes through a series of transformations of the profile involving as an intermediate state a spatially varying slope in the vicinity of the contour line  $\phi = \frac{1}{2}$  defining the interface position. Even after a time of  $t \approx 30 W^4/M$ , while near the interface position the profile is well-behaved and has the right width, there are still indentations in it far from the interface, and these disappear only slowly.

While the LCT model keeps a nicer profile all the time, it relaxes only slowly as well. Moreover, if the boundary

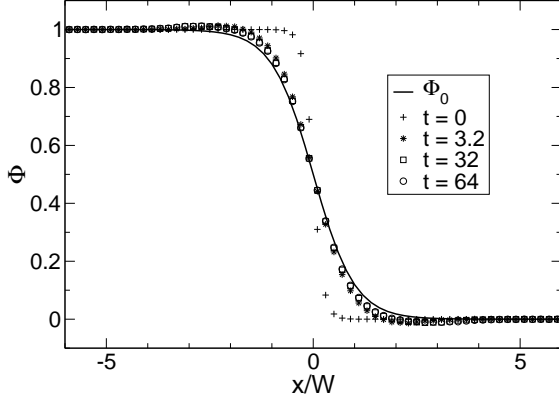


FIG. 8: Relaxation towards the correct interface profile for the LCT model. The initial interface width is  $0.25 W$ , the time  $t$  is given in units of  $W^4/M$ .

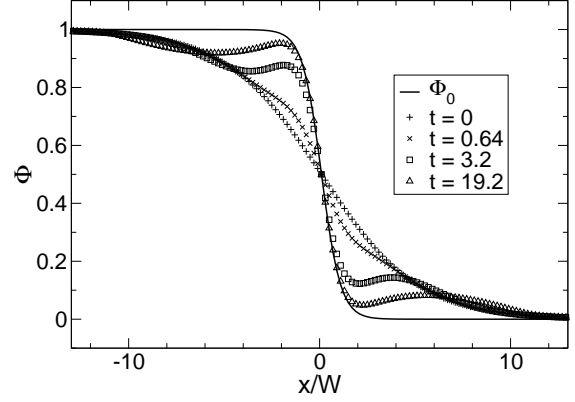


FIG. 10: Relaxation towards the correct interface profile for the SM model. The initial interface width is  $5 W$ , the time  $t$  is given in units of  $W^4/M$ .

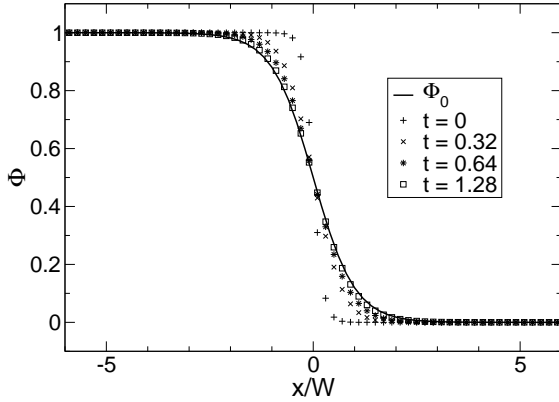


FIG. 9: Relaxation towards the correct interface profile for the GCT model. The initial interface width is  $0.25 W$ ,  $N = 1.25 M/W^2$ , the time  $t$  is given in units of  $W^4/M$ .

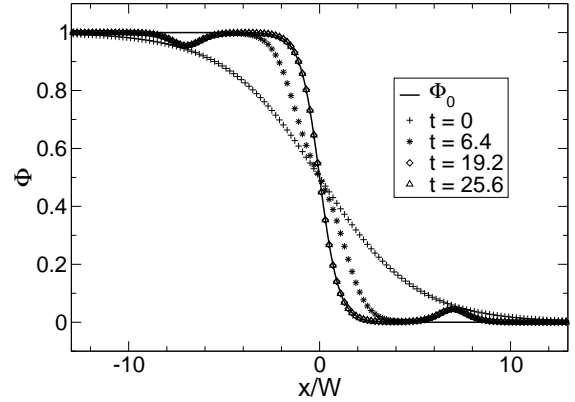


FIG. 11: Relaxation towards the correct interface profile for the RRV model. The initial interface width is  $5 W$ , the time  $t$  is given in units of  $W^4/M$ .

values of  $\phi$  are not fixed to be equal to zero or one, it will relax to constant values in the bulk different from these ideal values (in the absence of elasticity). Indeed, inspection of Eq. (64) shows immediately that any constant value of  $\phi$  solves the bulk equations of motion. (This is no longer true in the presence of elasticity.) For phases extending to the system boundary, the value of the constant is only fixed by the boundary conditions. Therefore, the model should always be run with Dirichlet boundary conditions for the phase field. (Due to the conservation law, inclusions of one phase in another will keep their  $\phi$  value, even in the presence of elasticity, if correctly initialized to zero or one, as long as their inner volume is much larger than that of their interface.) Performing

such a simulation, we found relaxation to be as slow as for the SM and RRV models but the interface profile to look more reasonable.

To summarize, when interface thickness is believed to be an issue in simulations, i.e., when there are reasons to think that it might vary considerably (which may be the case when surface tension anisotropy is included in the model), the nonexact realization of the conservation law by the GCT model may turn out a virtue rather than a drawback, since changes in the direction normal to the interface by diffusion only, as realized in the other models, tend to be too slow.

Finally, we compare the different dynamics for a "real-life" situation of an elliptical inclusion that morphs into

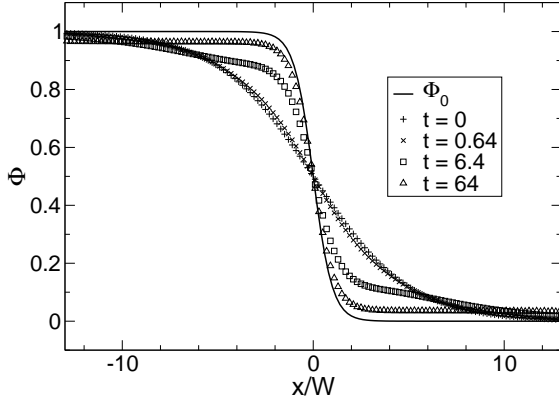


FIG. 12: Relaxation towards the correct interface profile for the LCT model. The initial interface width is  $5W$ , the time  $t$  is given in units of  $W^4/M$ .

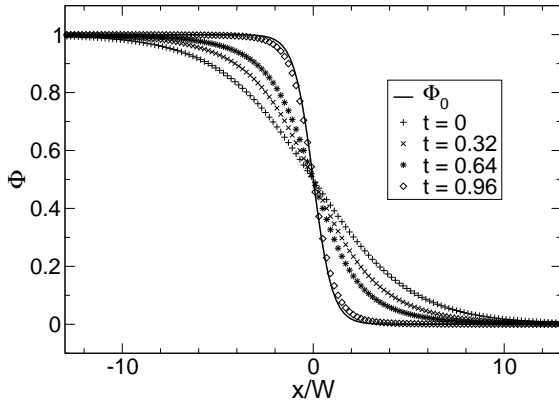


FIG. 13: Relaxation towards the correct interface profile for the GCT model. The initial interface width is  $5W$ , the time  $t$  is given in units of  $W^4/M$ .

a circle without elastic effects,  $F = 0$ . The system is initialized with a sharp interface ellipse with semimajor  $a_0$  and semiminor  $a_0/2$  and is then allowed to relax for a few time steps running the GCT-model (with a Lagrange multiplier  $\Lambda = 0$ ), in order to obtain an initial condition with the correct interface width everywhere. We then measure the time evolution of the semimajor and semiminor of the ellipse, continuing the run with the model to be studied.

As Fig. 14 shows, all models but the SM-model converge to a circle with the correct radius  $\sqrt{2}a_0/2$ . The SM-model shows different behavior, namely a too small radius that seems to decrease further. Since the phase field is a conserved quantity (we also checked that numerically

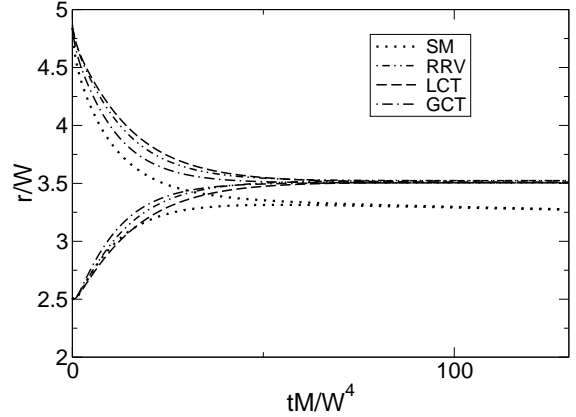


FIG. 14: Comparison of the time development of the size of an elliptical inclusion. The square system had the length  $L/W = 20$ . The initial ellipse had a semimajor of  $a_0 = L/4$  and a semiminor of  $L/8$ . All models except the SM-model converge to circles with the same radius  $r$ .

for our code), this can only mean that the final shape of the inclusion is not a true circle but a slightly deformed one, displaying a certain level of anisotropy. We then increase the size of the system and the included ellipse while keeping the interface width constant, resulting in a better scale separation  $a_0/W$ . While for the LCT-, GCT- and RRV- model the curves collapse onto a single line, this is not the case for the SM-model. Fig. 15 demonstrates this behavior for the LCT-model. The comparison for the SM-model is shown in Fig. 16.

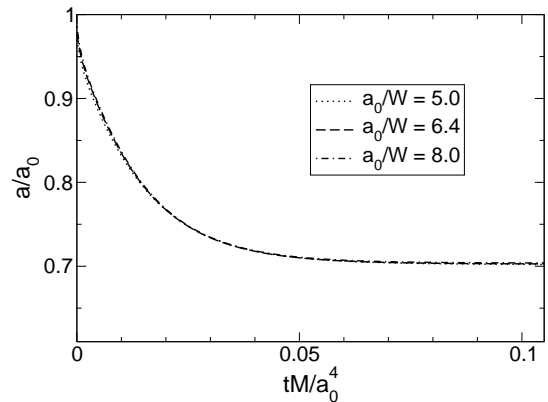


FIG. 15: Elliptical inclusion: comparison of the time development of the length of the semimajor  $a$  for the LCT-model. The initial length is denoted by  $a_0$  and the different curves correspond to different scale separations  $a_0/W$ . All curves collapse onto a single line.

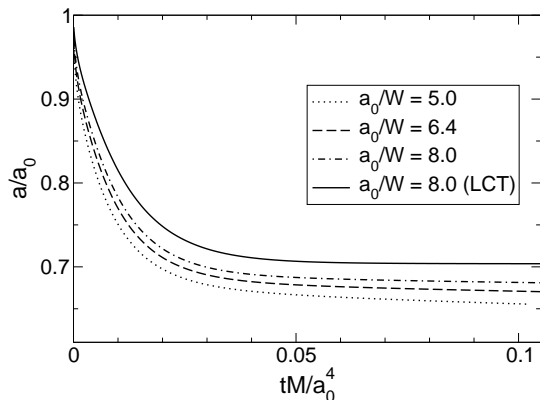


FIG. 16: Elliptical inclusion: comparison of the time development of the length of the semimajor  $a$ . The initial length is denoted by  $a_0$  and the different curves correspond to different scale separations  $a_0/W$ . The performance of the SM model becomes asymptotically better for larger systems. Results for the LCT-model have been included as a reference.

### VIII. CONCLUSIONS

The intuitive approach to constructing a phase-field model for surface diffusion consists in using the chemical potential known from the nonconservative model to define a current, involving its gradient and a mobility that vanishes in the bulk phases, and in taking the divergence of this current as the time derivative of the phase field. As has been shown in this article, this approach – the SM model – fails to produce the correct asymptotics in a subtle way. It does reproduce the equilibrium limit correctly and it appears to work numerically, although less efficiently than the alternatives discussed.

We offer a simple argument why the SM model should not be expected to work properly: The chemical potential functional of the model is constructed so that the chemical potential vanishes in the bulk phases. As the diffusion operator is essentially a scalar, diffusion acts also orthogonally to the interface; in its vicinity, the effect is even strong, because the slope of the phase field is largest in the direction perpendicular to the corresponding level set. This diffusive effect constitutes a driving force for relaxation of the chemical potential towards zero also close to the interface (asymptotically, the chemical potential *is* zero at next-to leading order). Surface diffusion of the chemical potential is then not the only effect contributing to the interface dynamics.

The RRV model avoids this problem by leaving the chemical potential in the bulk undetermined. Absence of diffusion in the bulk is not guaranteed by the chemical potential but by the vanishing mobility. Since the bulk chemical potential is free to vary, a true interface chemical potential can build up, the surface diffusion of which governs the interface dynamics.

Our contribution in this article is to explore the idea that the failure of the SM model might be remedied instead by making the mobility a tensor. After all, surface diffusion may be interpreted as highly anisotropic three-dimensional diffusion with a diffusion tensor that has zero eigenvalue in one direction. Whereas the pre-existing RRV model has the correct asymptotics, it does not exploit that idea. A straightforward attempt of its realization however fails in a rather drastic way, because restricting diffusion to the surfaces of constant phase field does not impose any functional dependence of  $\phi$  in the normal direction given by this foliation.

Modifying the tensorial mobility, one obtains the LCT and GCT models, both exhibiting the correct asymptotic behavior.

An analytic linear stability analysis of a planar front demonstrates that these two models reproduce the correct dispersion relation for local perturbations of the profile corresponding to a modified interface position. The phase-field dispersion relation is even free of corrections due to the front width. A similar analysis turns out infeasible for the SM model, while it could in principle be completed numerically for the RRV model (after analytic reduction to an ordinary differential equation).

Numerical study of the four models suggests that whereas the SM model has a range of quantitative validity (despite its not being asymptotic), and the RRV model is definitely viable, the modified tensorial models discussed here are probably more useful for large-scale simulations, as they permit larger time steps.

A possible way to understand this is as follows. In the scalar-mobility models (SM and RRV), the inner equation determining the interface velocity appears only three orders in  $W$  after the leading order. A simulation must of course represent the full model equations. Suppose we wish the interface velocity to be determined with an error not exceeding order  $W$ . Then the leading-order equation must be simulated with an accuracy  $O(W^4)$  at least. If one takes a simple second-order accurate discretization for the gradient operators in the equations, the numerical error due to discretization alone will be  $O(\Delta x^2)$  for a grid spacing  $\Delta x$ . To keep this smaller than  $W^4$ ,  $\Delta x$  would have to scale with  $W^2$ , which can be expected to lead to large computation times. Therefore, in the scalar mobility models, high-accuracy discretizations are mandatory, even when the asymptotic error is controllable, as is the case for RRV.

On the other hand, in the LCT and GCT models, discussed in Secs. VA and VB, as soon as the phase-field profile is represented with an error of order  $W$  or better, the effective leading order is only one order lower than the one determining the interface velocity, similar to the nonconservative case. Hence, reasonable accuracy should be attainable with grid spacings that scale as  $W$ , not as  $W^2$ . None of the benefits of high-accuracy discretizations would be lost to the need of representing terms very accurately that are very small in the leading-order equation.

Generally speaking, the most efficient model in terms

of computational cost is the LCT model. However, it is slowest in terms of “real” time (though not in terms of the number of time steps), when it comes to the relaxation from a wrong width of a planar interface to the correct value. This may be seen as a signature that the model is most efficient in suppressing diffusion perpendicular to the interface. In optimally initialized simulations, interface width variations arise gradually, via curvature changes and/or orientation changes (in models with anisotropic surface tension) and one should expect their relaxation via diffusion *along* the interface to be sufficiently efficient. Nevertheless, this property of the LCT model reduces its robustness as a numerical tool.

This is why we suggest the GCT model as an alternative that seems to be more accurate in most applications than the LCT model and digests variations of the interface width more easily than all the other models. Both accuracy and robustness of the GCT model, connected with its still favorable efficiency and simplicity of implementation, should make it the approach of choice in most cases.

**Acknowledgments** We wish to thank E. Brener and H. Müller-Krumbhaar for stimulating discussions that have led, among other things, to the introduction of a Lagrange parameter into the GCT model. Support of this work by DFG grants KA 672/9-1 and MU 1170/6-1, and the U. S. Department of Energy, Office of Basic Energy Sciences, through the Computational Materials Science Network program is gratefully acknowledged.

## APPENDIX A: MATCHING CONDITIONS

Let  $\tilde{\psi}(x, z, t) = \psi(r, s, t)$  be some arbitrary (sufficiently often differentiable) function of space and time obtained in solving the outer equations. We write the corresponding function of the inner solution as  $\Psi(\rho, s, t)$ , and suppress from now on, in this section, the dependence of functions on  $s$  and  $t$ . Moreover, we write the coefficient functions in expansions with respect to  $W$  with simple subscripts indicating their order rather than superscripts in parentheses as in the main text. There, the notation is dictated by the fact that a subscript would interfere with certain other subscripts; here, a superscript would interfere with the primes denoting derivatives.

We must have the asymptotic relationship

$$\Psi(\rho) \sim \psi(r) = \psi(W\rho) \quad (\rho \rightarrow \infty, W \rightarrow 0, W\rho \rightarrow 0). \quad (\text{A1})$$

Expanding both functions in powers of  $W$ , we get

$$\Psi(\rho) = \Psi_0(\rho) + W\Psi_1(\rho) + W^2\Psi_2(\rho) + \dots, \quad (\text{A2})$$

$$\begin{aligned} \psi(W\rho) &= \psi_0(r) + W\psi_1(r) + W^2\psi_2(r) + \dots \\ &= \psi_0(0) + W[\rho\psi'_0(0) + \psi_1(0)] \\ &\quad + W^2[\rho^2\frac{1}{2}\psi''_0(0) + \rho\psi'_1(0) + \psi_2(0)] + \dots, \end{aligned} \quad (\text{A3})$$

where the derivatives are to be taken for  $r \rightarrow +0$ , should they be discontinuous at  $r = 0$ . Analogous expressions with  $r \rightarrow -0$  are obtained for the asymptotics as  $\rho \rightarrow -\infty$ .

Equating powers of  $W$ , we then successively get the asymptotic relationships

$$\lim_{\rho \rightarrow \pm\infty} \Psi_0(\rho) = \psi_0(\pm 0), \quad (\text{A4})$$

$$\Psi_1(\rho) \sim \rho\psi'_0(\pm 0) + \psi_1(\pm 0) \quad (\rho \rightarrow \pm\infty), \quad (\text{A5})$$

$$\Psi_2(\rho) \sim \frac{1}{2}\rho^2\psi''_0(\pm 0) + \rho\psi'_1(\pm 0) + \psi_2(\pm 0) \quad (\rho \rightarrow \pm\infty). \quad (\text{A6})$$

Moreover, asymptotic relations such as (A5) can be decomposed into statements about function limits

$$\lim_{\rho \rightarrow \pm\infty} \partial_\rho \Psi_1(\rho) = \psi'_0(\pm 0), \quad (\text{A7})$$

$$\lim_{\rho \rightarrow \pm\infty} [\Psi_1(\rho) - \rho\psi'_0(\pm 0)] = \psi_1(\pm 0). \quad (\text{A8})$$

## APPENDIX B: USEFUL PROPERTIES OF THE PHASE FIELD FUNCTIONS

In order to simplify it for the reader to find the actual relationships for the various functions involving the phase-field that are used in the text, they are collected here for reference (and concreteness). Often only certain properties but not the precise form of these functions are important.

The chosen double-well potential is

$$f(\phi) = \phi^2(1 - \phi)^2. \quad (\text{B1})$$

Its derivative is given by

$$f'(\phi) = 2\phi(1 - \phi)(1 - 2\phi), \quad (\text{B2})$$

its second derivative reads

$$f''(\phi) = 2[1 - 6\phi(1 - \phi)]. \quad (\text{B3})$$

Let us define another function  $h(\phi)$ , which turns out useful, by

$$h(\phi) = \phi^2(3 - 2\phi), \quad (\text{B4})$$

having the derivative

$$h'(\phi) = 6\phi(1 - \phi). \quad (\text{B5})$$

To solve the ordinary differential equation satisfied by the zeroth-order inner solution

$$\partial_{\rho\rho}\Phi^{(0)} - 2f'(\Phi^{(0)}) = 0, \quad (\text{B6})$$

with boundary conditions  $\lim_{\rho \rightarrow -\infty} \Phi^{(0)}(\rho) = 1$  and  $\lim_{\rho \rightarrow \infty} \Phi^{(0)}(\rho) = 0$ , we multiply by  $\partial_\rho \Phi^{(0)}$ , integrate and take the square root (with the correct sign) to obtain

$$\partial_\rho \Phi^{(0)} = -2\Phi^{(0)}(1 - \Phi^{(0)}) = -\frac{1}{3}h'(\Phi^{(0)}), \quad (\text{B7})$$

which can be solved by separation of variables. The solution is, up to a translation in  $\rho$ , given by

$$\Phi^{(0)} = \frac{1}{2}(1 - \tanh \rho). \quad (\text{B8})$$

Requiring the position of the interface to be at  $\rho = 0$  fixes the choice out of the one-parameter set of solutions, present due to the translational invariance of the differential equation.

With the help of the second equality of (B7), it is easy to calculate certain integrals appearing in the asymptotic analysis. Those integrals typically contain the factor  $(\partial_\rho \Phi^{(0)})^2$ ; to do the integral, it is then beneficial to replace one of the factors (and only one) with  $-h'(\Phi^{(0)})/3$ . Integrals obtained this way have the structure

$$\begin{aligned} I &= \int_{-\infty}^{\infty} d\rho f(h(\Phi^{(0)})) (\partial_\rho \Phi^{(0)})^2 \\ &= -\frac{1}{3} \int_{-\infty}^{\infty} d\rho f(h(\Phi^{(0)})) h'(\Phi^{(0)}) \partial_\rho \Phi^{(0)} \\ &= -\frac{1}{3} \int_1^0 d\Phi^{(0)} f(h(\Phi^{(0)})) h'(\Phi^{(0)}) \\ &= \frac{1}{3} \int_0^1 dh_0 f(h_0). \end{aligned} \quad (\text{B9})$$

This way, one arrives, for example, at

$$\int_{-\infty}^{\infty} (\partial_\rho \Phi^{(0)})^2 d\rho = \frac{1}{3}. \quad (\text{B10})$$

In the RRV model [24], we have to evaluate two more integrals, namely

$$\begin{aligned} \int_{-\infty}^{\infty} g(\Phi^{(0)}) \partial_\rho \Phi^{(0)} d\rho &= -\int_0^1 10x^2(1-x)^2 dx = -1/3, \\ \int_{-\infty}^{\infty} B(\Phi^{(0)}) d\rho &= \int_{-\infty}^{\infty} 3(\partial_\rho \Phi^{(0)})^2 = 1. \end{aligned} \quad (\text{B11})$$

### APPENDIX C: DETAILS OF THE ANALYTIC LINEAR STABILITY CALCULATION

In the nonconservative case, the eigenvalue problem to be solved reads

$$\omega \Psi = \frac{M}{W^2} (\partial_{zz} - W^2 k^2 - 2f''(\Phi_0)) \Psi. \quad (\text{C1})$$

This may be considered the inner problem, given in the coordinates  $(x, Z)$ , with  $Z = z/W$ . Setting  $\psi(z) = \Psi(Z)$ , the corresponding outer problem reads:

$$\omega \psi = M \left( \partial_{zz} - k^2 - \frac{4}{W^2} \right) \psi, \quad (\text{C2})$$

where we have used  $\lim_{Z \rightarrow \pm\infty} f''(\Phi_0) = 2$  [see (B3)]. Using the expansions

$$\begin{aligned} \omega &= \frac{\omega_{-2}}{W^2} + \frac{\omega_{-1}}{W} + \omega_0 + \omega_1 W + \dots \\ \Psi(Z) &= \Psi_0(Z) + W \Psi_1(Z) + W^2 \Psi_2(Z) + \dots \\ \psi(z) &= \psi_0(z) + W \psi_1(z) + W^2 \psi_2(z) + \dots \end{aligned} \quad (\text{C3})$$

we then have, at leading order

$$\omega_{-2} \psi_0 = -4M \psi_0 \quad (\text{C4})$$

meaning that either  $\omega_{-2} = -4M$  or  $\psi_0 \equiv 0$ . Thus we have to distinguish two cases.

If  $\omega_{-2} = -4M$ , the lowest-order inner equation becomes

$$\Psi_0''(Z) + \frac{6}{\cosh^2 Z} \Psi_0(Z) = 0, \quad (\text{C5})$$

where we have used (B8). This is a one-dimensional Schrödinger equation that can be reduced to Legendre's differential equation [32] via the substitution  $u = \tanh Z$  and hence is exactly solvable. In this particular case, the solution that remains finite at infinity is the second-order (in  $u$ ) Legendre polynomial

$$\Psi_0(Z) = \frac{1}{2} (3 \tanh^2 Z - 1). \quad (\text{C6})$$

This means that the perturbation is not localized – it does not approach zero for  $Z \rightarrow \pm\infty$ . As usual, once the zeroth-order solution has been found, perturbation theory can be carried through without major difficulties, inserting the expansions (C3) into (C1) and (C2). Calculating the eigenvalue to zeroth order in  $W$ , we find  $\omega_a$  from (83). In fact, continuing the calculation to higher orders, we note that no additional contributions to  $\omega_a$  arise. The suspicion that (C6) is an exact solution – and  $\omega_a$  the corresponding exact eigenvalue – to Eq. (C1) is confirmed by backsubstitution into the equation.

The second solution is obtained by assuming  $\omega_{-2} = 0$  and, hence,  $\psi_0(z) = 0$  in the outer region. This gives the leading-order inner equation

$$\Psi_0''(Z) - 2f''(\Phi_0) \Psi_0(Z) = 0, \quad (\text{C7})$$

the relevant solution of which we know already, because the linear operator acting here is just  $\mathcal{L}$  from (39) with the role of  $\rho$  taken by  $Z$ . Hence

$$\Psi_0(Z) = \Phi_0'(Z) = -\frac{1}{2 \cosh^2 Z}, \quad (\text{C8})$$

which is a solution localized about the interface and approaching zero for  $Z \rightarrow \pm\infty$ . Inserting the expansions (C3) with the evaluated results for  $\omega_{-2}$ ,  $\psi_0(z)$  and  $\Psi_0(Z)$  into (C1) and (C2), we find that the eigenvalue is to all orders given by  $\omega_b$  from (83) and that, in fact,  $\Psi_0(Z)$  and  $\omega_b$  constitute an exact solution to the eigenvalue problem. There may be more admissible solutions, but for all of them  $\omega$  should be negative and diverge more strongly than  $1/W^2$  for  $W \rightarrow 0$ , so they will not be relevant in the limit of small  $W$ .

- 
- [1] S. Osher and J. A. Sethian *J. Comp. Phys.*, **79**, 12 (1988).
- [2] J. A. Sethian, *Level Set Methods and Fast Marching Methods: Evolving Interfaces in Computational Geometry, Fluid Mechanics, Computer Vision, and Materials Science* (2nd ed.), Cambridge University Press (1999).
- [3] A. Karma and W.-J. Rappel, *Phys. Rev. E* **53**, R3017 (1996).
- [4] A. Karma and W.-J. Rappel, *Phys. Rev. E* **57**, 4323 (1998).
- [5] J. S. Langer and R. F. Sekerka, *Acta Metall.* **23**, 1225 (1975).
- [6] J. B. Collins and H. Levine, *Phys. Rev. B* **31**, 6119 (1985).
- [7] G. Caginalp and P. Fife, *Phys. Rev. B* **33**, 7792 (1986).
- [8] G.B. McFadden, A.A. Wheeler, R.J. Braun, and S.R. Coriell, *Phys. Rev. E* **48**, 2016 (1993).
- [9] R. Kobayashi, *Physica D* **63**, 410 (1993).
- [10] R. Kobayashi, *Exp. Math.* **3**, 60 (1994).
- [11] T. Abel, E. Brener, and H. Müller-Krumbhaar, *Phys. Rev. E* **55**, 7789 (1997).
- [12] A.A. Wheeler, G.B. McFadden, and W.J. Boettinger, *Proc. Roy. Soc. Lond. A* **452**, 495 (1996).
- [13] H. Garcke, B. Nestler, and B. Stoth, *SIAM J. Appl. Math.* **60**, 295 (1999).
- [14] O. Pierre-Louis, *Phys. Rev. E* **68**, 021604 (2003).
- [15] F. Otto, P. Penzler, A. Rätz, T. Rump, A. Voigt, *Nonlinearity* **17**, 477 (2004).
- [16] J. Müller and M. Grant, *Phys. Rev. Lett.* **82**, 1736 (1999).
- [17] K. Kassner and C. Misbah, *Europhys. Lett.* **46**, 217 (1999).
- [18] K. Kassner, C. Misbah, J. Müller, J. Kappey, P. Kohlert, *Phys. Rev. E* **63**, 036117 (2001).
- [19] M. Grinfeld, *Sov. Phys. Dokl.* **31**, 831 (1986).
- [20] R. Asaro and W. Tiller, *Metall. Trans.* **3**, 1789 (1972).
- [21] W. H. Yang and D. J. Srolovitz, *Phys. Rev. Lett.* **71**, 1593 (1993).
- [22] K. Kassner and C. Misbah, *Europhys. Lett.* **28**, 245 (1994).
- [23] M. Haataja, J. Müller, A.D. Rutenberg, M. Grant, *Phys. Rev. B* **65**, 165414 (2002).
- [24] A. Rätz, A. Ribalta, A. Voigt, *J. Comp. Phys.* **214**, 187 (2006).
- [25] D.-H. Yeon, P.-R. Cha, M. Grant, *Acta Materialia* **54**, 1623 (2006).
- [26] J.W. Cahn, C.M. Elliott, A. Novick-Cohen, *Euro. J. Appl. Math.* **7**, 287 (1996).
- [27] M. Mahadevan and R.M. Bradley, *Physica D* **126**, 201 (1999).
- [28] D.N. Bhate, A. Kumar, and A.F. Bower, *J. Appl. Phys.* **87**, 1712 (2000).
- [29] K. Kassner, *How to model surface diffusion using the phase-field approach*, cond-mat/0607823
- [30] M.A. Spivak, *Comprehensive Introduction to Differential Geometry*, Vol. 3, 2nd ed. Publish or Perish, Inc., Wilmington, Del., 1979.
- [31] R. Spatschek, C. Müller-Gugenberger, E. Brener, and B. Nestler, *Phys. Rev. E* **75**, 066111 (2007).
- [32] M. Abramowitz, I. Stegun, *Handbook of Mathematical Functions*, Dover, New York (1972).